# CHARACTERIZATION OF MEMBRANE VISCOSITY CHANGES WITH THE NOVEL MOLECULAR ROTOR FCVJ

---

A thesis presented to the Faculty of
the Graduate school at the
University of Missouri-Columbia

---

In Partial Fulfillment
of the Requirements for the Degree

Master of Science

---

by

MATTHEW E. NIPPER

Dr. Mark Haidekker, Thesis Advisor

AUGUST 2007

The undersigned, appointed by the dean of the Graduate School, have examined the thesis

entitled

CHARACTERIZATION OF MEMBRANE VISCOSITY
CHANGES WITH THE NOVEL MOLECULAR ROTOR FCVJ

presented by Matthew E. Nipper,

a candidate for the degree of master of science,

and hereby certify that, in their opinion, it is worthy of acceptance.

Dr. Mark Haidekker, Biological Engineering

Dr. Gerald Meininger, Medical Pharmacology and Physiology

Dr. Shinghua Ding, Biological Engineering

ACKNOWLEDGEMENTS

I would like to thank Dr. Mark Haidekker for supporting this project. Without his help and guidance this project would not have been possible. I would also like to thank Darcy Lichlyter, Jacob Hicks, and Dr. James Lee for their help with the liposome formation and imaging portion of this project. I also extend a great thanks to my committee members Dr. Gerald Meininger and Dr. Shinghua Ding for their suggestions and input.

TABLE OF CONTENTS

LIST OF FIGURES

LIST OF TABLES

Table Page

CHARACTERIZATION OF MEMBRANE VISCOSITY

CHANGES WITH THE NOVEL MOLECULAR ROTOR FCVJ

Matthew E. Nipper

Dr. Mark Haidekker, thesis supervisor

ABSTRACT

Membrane viscosity conditions are a useful indicator of cell viability. Atherosclerosis, Alzheimer's disease, diabetes mellitus, and hypertension have all been reported to induce changes in afflicted cell membrane viscosity. Characterizing membrane viscosity will provide researchers and clinicians with a valuable tool in diagnosing the onset and progression of diseases. Molecular rotors are fluorescent molecules that have been shown to exhibit viscosity sensitive quantum yield. The Forster-Hoffman equation, $\log\Phi=C+X\log\eta$, relates the quantum yield $\Phi$, of the rotor to the microviscosity state, $\eta$, present. According to this equation, increased viscosity will produce corresponding increased intensity values following a power law relation.

The phospholipid DLPC (1, 2-Dilauroyl-sn-Glycero-3-Phosphocholine) was combined with 10 μL of the molecular rotor FCVJ and liposomes were formed using an electroformation process. 250mM Sucrose solution served as the liposome formation solution. Control solutions of 50 ul of liposomes were then added to 950 μL of Sucrose solution in a microcuvette. The cuvette was excited at 460 nm under fluorescent spectroscopy and intensity values were recorded. The procedure was repeated for a 2% cyclohexane/sucrose solution. Peak emissions were compared and, as hypothesized, the cyclohexane fluidized the membrane resulting in a statistically significant reduction in

intensity compared to the control group (p=.00001, n=10). To achieve a converse effect, a 20% (v/v) Cholesterol/DLPC mixture was used to produce liposomes in the presence of sucrose solution. Total FCVJ concentration remained constant. 50ul of the cholesterol liposomes were added to 950ul of the Sucrose solution. Excitation parameters were kept constant. Intensity values were compared to those of the control group for the cyclohexane experiments. As expected, the intensity values for the cholesterol group were higher than control and found to be significant (p=.004, n=10).

The liposomes used in this experiment are a suitable model for the mammalian cell membrane in both size and physical similarities. The next evolution in this research is to test our hypothesis on animal cells in vitro. The results of these experiments demonstrate the high level of sensitivity and abilities of molecular rotors as microviscosity detectors. This previously undocumented method for characterizing membrane conditions provides a qualitative method of measuring changes in membrane viscosity.

# CHAPTER 1

## Definition and Role of Membrane Viscosity

Viscosity is classically defined as an isotropic fluid's resistance to flow. This property determines the fluid strain rate generated by an applied shear stress [1]. Viscosity, along with the inverse; fluidity, have been adapted by membrane biologists to qualitatively describe the characteristics of the lipid bilayer. A general consensus has been reached that viscosity determines the ease of movement for a particle in the two dimensional realm of the membrane bilayer [2]. There has been some discussion over the role of particle size in the debate. It has been argued that a small particle would react drastically to minute changes in microviscosity, whereas larger particles would be insensitive to small changes in local viscosity [2]. Regardless, membrane viscosity is an important parameter that affects organisms at both the cellular and systemic levels. An in depth look at the cellular membrane reveals the significance of membrane viscosity.

Membrane viscosity primarily governs the ability of intermembrane particles to travel laterally through the bilayer. The ability of these particles, such as membrane bound proteins, to move through the membrane plays an intrinsic role in their function [3,4]. Thus, a change in membrane viscosity can often be indicative of a disease state within a cell [5-8]. Membrane viscosity changes have all been reported with the onset of cell malignancy [3], diabetes [9,10], hypercholesterolemia [9] and atherosclerosis [8].

An in-depth look at atherosclerosis reveals that the role of membrane viscosity is complex and far reaching. One key pathway leading to atherosclerosis is the reduction of endothelium-derived relaxing factor/nitric oxide (EDRF/NO) from the cell membrane.

Cholesterol is believed to modulate the production of EDRF by means of membrane viscosity [11]. The effects of cholesterol on membrane viscosity of bovine aortic cells were investigated with the fluorescent probe 1,6-diphenyl-1,3,5-hexatriene (DPH) [11]. This technique will be discussed in the following chapter. Low amounts of cholesterol were found to cause both a slight increase in membrane viscosity and a higher production of EDRF. It is believed that small amounts of cholesterol increase enzyme production by increasing conformational flexibility on nitric oxide synthase. On the contrast, high amounts of cholesterol drastically increased membrane viscosity while significantly lowering EDRF production. The high membrane viscosity is believed to impair membrane protein production [11].

This effect was observed to be reversible, suggesting that the effects caused by cholesterol were mechanical and not a chemical modulation of membrane proteins [11]. Membrane mechanics play in an intrinsic role in the physiological processes of endothelium cells as well as erythrocytes.

An increase in membrane viscosity has been reported in both the erythrocytes and platelets of patients afflicted with diabetes. It has been suggested that this increase in membrane viscosity may perturb the ability of insulin, a membrane bound receptor, to undergo aggregation [10,12]. Erythrocytes of patients suffering from liver disorders have also been reported to exhibit higher membrane viscosity and it is believed that this contributes to liver dysfunction [13]. Additional increases in membrane viscosity of leukocytes have been linked with aging [14].

Conversely, decreases in membrane viscosity have been exhibited in the leukocytes of patients with Alzheimer's disease [15]. This decrease may facilitate the aggregation of the amyloid precursor protein which leads to the formation of plaques within the brain [15]. The formation of plaques are the primary mechanism responsible for the decline in cognitive abilities in patients with Alzheimer's disease. It is evident that membrane viscosity measurement provides a wealth of information about cell condition. The relationships between these diseases and membrane viscosity is not fully understood. To better understand these interactions, the properties and functions of the plasma membrane must first be considered.

The plasma membrane of a eukaryotic cell is one of the most crucial components of the cell. The most basic function of the membrane is to separate the intracellular components from the extracellular environment. A eukaryotic cell is depicted in Figure 1.

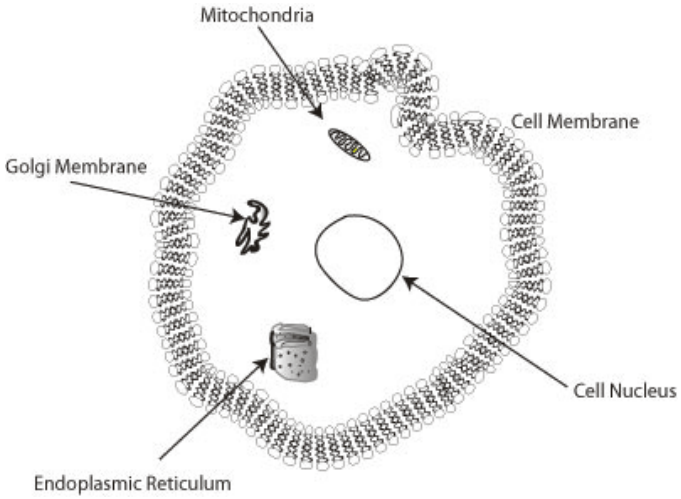


**Figure 1** - Eukaryotic Cell

The plasma membrane also has a central role in active transport, cell recognition, and overall metabolism of the cell.

The functions of the human erythrocyte are an excellent example of the metabolic properties of the plasma membrane. With no intracellular organelles, this provides an excellent model studying the role of membranes in metabolic processes. Erythrocytes are responsible for carrying glucose throughout the body. The absorption of glucose into the cell is governed by an intermembrane bound glucose transport protein. The ability of a red blood cell to absorb glucose is drastically reduced if the glucose transport protein is mechanically hindered [2]. Along with intermembrane proteins, ion channels also play a central role in metabolic processes.

Ion channels located within the plasma membrane surface are responsible for rapid change in the chloride-bicarbonate gradient. The fast acting abilities of the ion channel allow for high rates of anion flux. Anion flux plays a pivotal role in the binding and absorption of oxygen by hemoglobin and in $CO_2$ transport. The rapid anion flux allows for intermembrane proteins such as Na/K pumps to perform ATP production in the cell. Not only is the membrane for intracellular processes, the membrane also plays a role in intercellular communication.

Cell-cell communication is fundamental to cell division and differentiation. The building of complex organ systems relies on the ability to identify the correct matrix and building of the structure which is dictated by genetic information. The cell-cell and cell-matrix recognition abilities of the cell arise from proteins imbedded within the plasma

membrane. If these recognition systems are not operational, cell growth and division can grow uncontrollably which is characteristic of tumor cells [2,11].

Plasma membranes can form very tight connections between cells where the intercellular space is so small it can not be distinguished with electron microscopy [2]. This tight formation of layers are found in epithelial tissue so as to form a sealed layer. The plasma membrane then controls the transport of materials through the barrier. The recognition systems of cells are highly developed and do not require direct contact to be established.

On the other hand, Cells can also communicate with each other by forming gap junctions. These junctions are hollow protein tubes that extend out of the membrane and bridge gaps of 20-40 Å [2]. These tubes facilitate the rapid flux of ions and in turn provide a sort of communication. Such gap junction systems are found in involuntary muscle where fast ion flux is essential for proper function. Cell-cell communication is also controlled by cell recognition receptors found on the surface of the membrane.

There are a number of integrated carbohydrates present on the surface of the plasma membrane. This coat of glycoproteins and glycolipids present on the membrane surface are secreted by the cell to form a protective coating called the glycocalyx. In addition to cell-cell communication, the glycocalyx offers a mean for cells to adhere to one another. The cell membrane is responsible for mass transport, protection and the upper level organization required to form tissues and organ systems.

The structure of the cell membrane is intrinsically simple yet versatile enough to regulate a variety of cellular functions. The hydrophobic effect is the driving force behind

membrane formation and this water interaction is key to understanding membrane structure. Water plays a central role in the formation of biological membranes. The hydrophobic effect refers to the formation of a water excluding bond between two non-polar substances in a polar (water) environment.

Water is unique in the fact that it can easily form hydrogen bonds with other polar molecules. This property comes from the polarity of the O-H bonds. The electronegativity difference between oxygen and hydrogen force the electrons to be asymmetrically distributed with a bias towards the oxygen nucleus. The oxygen portion carries a partial negative whereas the hydrogen portion carries a partial positive charge. The attractive forces then draw the hydrogen portion of one water molecule to the oxygen end of another water molecule. This results in the sharing of one hydrogen proton between two oxygen molecules. This occurrence is referred to as a hydrogen bond. This results in the water-water interaction being energetically favorable.

A neutral species is readily soluble into water due to the ability to both accept and donate electrons. An example of this is ethanol. As the ethanol enters the water, it both accepts and donates a hydrogen to the water. Ethanol is very accommodating to water and therefore readily soluble.

Nonpolar hydrocarbons react much differently with water. For example, a long chained hydrocarbon has no available hydrogens to donate nor can it accept any. This results a restructuring of the water network. In a normal solution water molecules are oriented randomly. With the introduction of a non-polar species, the water forms cages around the molecules and as a result the randomness, or entropy, decreases.

A change in entropy directly affects the free energy. Free energy change, $\Delta G$, is calculated by Equation 1 where $\Delta H$ is the enthalpy change, $T$ is the temperature, and $\Delta S$ is the change in entropy. Equation 1shows a negative entropy will lead to a larger free

$$\Delta G = \Delta H - T\Delta S \quad \textbf{(1)}$$

energy. This means that this is energetically unfavorable for the system. This entropic parameter will determine if a substance will be soluble in a solvent.

$$\mu_w = \mu_w^{\,o} + RT(\ln X_w) + RT(\ln f_w) \quad \textbf{(2)}$$

A relationship for the chemical potential for a hydrocarbon in water was derived by Tanford (1980) and is shown in Equation 2 [16]. In Equation 2 $X_w$ is the mole fraction of hydrocarbon and $f_w$ is the activity coefficient. This equation can predict the potential of the hydrocarbon in water. The reaction a hydrocarbon will have with water is also dependent on if the hydrocarbon is saturated. This equation can be used to predict the hydrophobicity between two species.

The hydrophobic effect is directly dependent on the hydrophobic area that is exposed to the aqueous environment. As the exposed area increases so do the unfavorable entropic conditions. The relationship between free energy and chain length increases linearly until chain lengths become very long. At this point it is believed that the long chain molecules form bonds within itself and folding begins [2]. This effectively reduces the hydrophobic area and thus the free energy change. Also aggregation begins to occur more frequently, effectively reducing the area of hydrophobic species being exposed to

water. It is because of this effect that phospholipids aggregate into the fundamental element of membranes; the phospholipid bilayer [2]. This is also the mechanism by which proteins are integrated into the membrane. The hydrophobic effect is a powerful entropic force that governs both the form and function of lipid bilayers.

Biological membranes can be formed by a variety of membrane lipids. Lipids are amphiphatic molecules that position their polar heads towards the water and their non-polar tails inward forming the hydrophobic core. The polar head is commonly a phosphate with an alcohol. The remaining tail portion is typically a saturated hydrocarbon tail.

Mammalian membranes are comprised of a number of phospholipid compositions. The order and composition of the phospholipids within the membrane can be used to detect physiological changes at the cellular level. One of the most common and extensively studied phospholipids is phosphatidylcholine. The structure of phosphatidylcholine is depicted in Figure 2 . This structure is also referred to as lecithin which comes from older nomenclature [2].

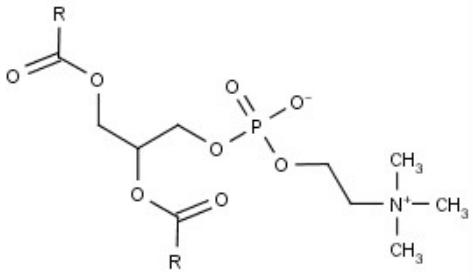


**Figure 2** - Chemical Structure of Phosphatidylcholine

In addition to phosphatidylcholine, there are a number of other phospholipids present within the membrane. The table below lists the mole percentage of phospholipids in a human erythrocyte along with the cholesterol content. The table below shows the lipid composition of a membrane is dynamic. The percentage of a lipid present in a membrane is often indicative of its function.

Table 1.1 - Lipid Composition and Cholesterol Content of Human Erythrocyte

| **Lipid** | **Mol%** |
|---|---|
| Phosphatidylcholine | 17 |
| Phosphatidylserine | 6 |
| Phosphatidylethanolamine | 16 |
| Sphingomyelin | 17 |
| Cholesterol | 45 |

Cholesterol is also present within the membrane and makes up the remaining fatty acids. Cholesterol is essential for life and proper cell function yet the negative side effects are often the first to be discussed [17]. Excess cholesterol can lead to the formation of plaques along the arterial wall. When the plaque blocks flow to the heart, heart muscle can die as a result. The heart attack that results can be deadly.

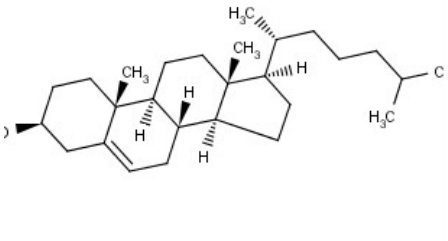


**Figure 3** - Chemical Structure of Cholesterol

The chemical structure of cholesterol is shown in Figure 3. The molecule is oriented in such a way that the polar hydroxyl group is positioned towards the aqueous environment. The hydrophobic rings are then oriented parallel to the hydrocarbon chains of the membrane. The ring structures present make the molecule extremely hydrophobic and thus solubility is greatly reduced. The structure is however readily accepted by membranes.

The cholesterol content has been shown to affect a wide range of physical parameters of the membrane. The effects that cholesterol has on the lipid bilayer is dynamic dependent on the length of the hydrocarbon tail portion of the membrane. Cholesterol can effectively increase the width of the membrane if the phospholipid tails are shorter than 16 carbons [2]. This forces the hydrocarbon tails to adopt more trans confirmations. The tail portions must consolidate at 18 carbons due to the fact that cholesterol is not as long, which effectively shrinks the membrane size [18].

Along with membrane size being affected, the membrane permeability is also highly correlated with cholesterol content. The effects of membrane permeability on

glucose transport through the membrane were investigated and it was found that a reduction in permeability followed an increase in cholesterol content in a linear fashion [19]. It is believed that the cholesterol may reduce imperfections in the membrane that arise from trans isomerizations which would lead to a reduction in permeability.

The trans isomerizations, referred to as kinks, are simply small pockets between the hydrocarbon chains that arise from the asymetrical confirmation. The reduction in kinks can be considered as a reduction in free volume. Free volume can be considered the amount of "defects" in the membrane that arise from kinks in the tails of the phospholipids in the membrane [2]. Free volume allows for the conformational changes necessary for membrane proteins to function properly. If the number of defects are decreased, so is the available space for proteins or other integral proteins to occupy. The amount of free volume is related to the local membrane viscosity [2].

The ability of cholesterol to regulate local free volume in the membrane is intrinsic to a host of physiological processes. The true purpose of cholesterol in the membrane is not well known. One known attribute of cholesterol is that it lowers the liquid-crystalline phase change temperature of the membrane and acts as an "antifreeze" for the membrane. It is understood that a cell can not function properly without the appropriate amount of cholesterol. There are some specific effects that have been observed in modulating cholesterol content.

Researchers have found that an increase in membrane cholesterol was responsible for an increase in membrane protein function. An increase was found for the Na+, K+, ATPase activity corresponding to a 0 to .35 mole ration [20]. The increase in cholesterol

lead to an increase of the ATP hydrolyzing activity. Other membrane functions have been shown to be minimally affected by alterations in cholesterol content. In the same experiment no alteration in sarcoplasmic reticulum Ca2+ ATPase activity was recorded [20].

There are two commonly hypothesized modalities by which these effects occur. The first is that the cholesterol is affected by the reduction in free volume. The limited space allows for fewer confirmations the membrane protein can achieve and thus limited function. The limitation in confirmations is also a function of temperature. This non-specific structural hindrance is in direct contrast to the other possible explanation.

Experiments suggest that some membrane proteins have a direct sterol binding site. This sterol-protein interaction has been reported in the integral membrane proteins glycophorin [21], and band 3 [22], from human erythrocytes. This type of interaction has been observed in water-soluble proteins. In a similar fashion, a specific binding site on the membrane protein would govern the sterol-protein interaction and in turn binding kinetics. A number of techniques have been developed to differentiate mechanical hindrance from biochemical modulation. By measuring intermembrane viscosity, changes in membrane function that result from disease or other interactions can be better understood.

Measuring membrane viscosity until recent years, has been an arduous task. A variety of mechanical methods have been developed to measure membrane viscosity. Common methods for measuring membrane viscosity include micropipette aspiration and magnetic microbeads.

Micropipette aspiration techniques have been used to investigate the effects of F-actin microfilaments on membrane viscosity of human Mesenchymal Stem Cells [23]. Stem cells were treated with cyctochalasin-D, a F-actin filament disrupter, and untreated stem cells were used as a control. Both groups were then aspirated with a known pressure. Figure 4 depicts the setup used in these experiments.

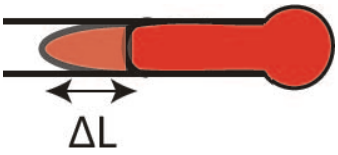


**Figure 4** - Aspirated Stem Cell

After reaching equilibrium, the pressure was increased in steps , $\Delta P$, ranging from 500 Pa to 1000 Pa. The aspirated length, $L$, was then measured with a CCD camera and bright field microscopy. Equation 3 relates the length of the aspirated portion of the cell, as a time dependent function, with the elastic parameters $k_1$ and $k_2$, the inner pipette radius $a$, and the time constant $\tau$. $\Phi$ is a dimension less parameter, with a value of 2.0, that accounts for the wall thickness of the pipette. This technique assumes a boundary condition of zero axial displacement at the micropipette end.

Using Equations 3 and 4, the elastic parameters $k_1$ and $k_2$, along with the apparent

$$L(t) = \frac{\Phi a \Delta P}{\pi k_1}\left[1 - \frac{k_2}{k_1 + k_2} e^{-t/\tau}\right] \quad \textbf{(3)}$$

$$\mu = \frac{\tau \cdot k_1 k_2}{k_1 + k_2} \quad \textbf{(4)}$$

viscosity $\mu$ can be calculated through nonlinear regression. The results of the experiment showed that with the treatment of cyctochalasin D, the average membrane viscosity of the experimental group increased 167% compared to control. The micropipette aspiration technique has also been used to investigate the mechanical properties of rat erythrocytes [24] and hepatocellular carcinoma cells [25].

Magnetic microbeads and optical tweezing methods have gained popularity over recent years. The maneuverability and the addition of functional groups to the microbeads have provided researchers with the ability to measure membrane viscosity at discrete locations on the cell. The viscoelastic properties of fibroblasts were explored by attaching magnetic microbeads to integrin receptors that lie in the cell membranes [26]. Non-magnetic latex beads are also attached to provide a spacial reference. When the magnetic force is applied, the beads exhibit a three-phasic creep response consisting of an elastic deformation, a stress relaxation, and a viscous flow. By measuring these parameters as a function of time, the membrane viscosity can be calculated. The experimental setup is shown in Figure 5.

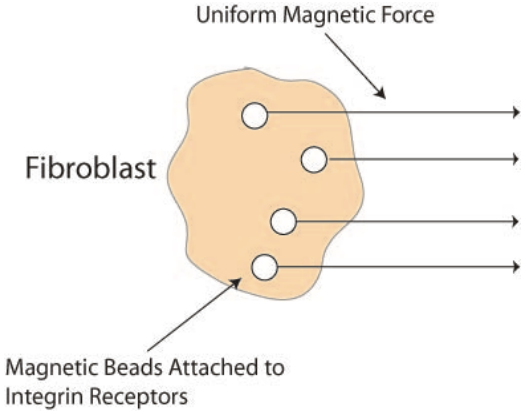


**Figure 5** - Magnetic Beads Attached to Integrin Receptors on a Fibroblast

Viscosities of 5-10 Pa•s and $2\times10^3$ Pa•s were found for the membrane and cytoplasm respectively. The membrane viscosity is nearly 1 order of magnitude lower than the found value for a red blood cell using pipette aspiration [27]. The cytoplasmic viscosity was in good agreement with values ranging from 250 to 2800 Pa•s for cytoplasmic viscosity of macrophages using twisting rheometry [28,29]. Magnetic particle rheometry has been shown to be effective yet obvious limitations exist.

A central problem to both of these methods is that the temporal and spatial resolution are poor and provide limited information about the membrane as a whole. The measurement is also observed at the outermost layer of the membrane, and the effects on the hydrophobic core are not discernible. Advances in fluorescent probes have introduced an entirely new approach for membrane viscosity measurement.

# CHAPTER 2

## Overview of Fluorescence

Luminescence is the emission of a photon from an electronically excited molecule. The light emission is either characterized as fluorescence or phosphorescence depending on the excited state involved [30]. Fluorescence is the return of an electron from an excited singlet state to the ground state, or lowest energy level. A fluorophore is any molecule that exhibits fluorescence under excitation.

Aromatic molecules are often fluorescent due to the electron sharing capabilities of the ring structures present. Quinine was historically the first identified fluorophore by German Astronomer Sir John Frederick William Herschel in 1845. Herschel reported on quinine fluorescence from observing the characteristic emission of blue light from the solution after being exposed to sunlight. Figure 6 shows common fluorescent aromatic molecules

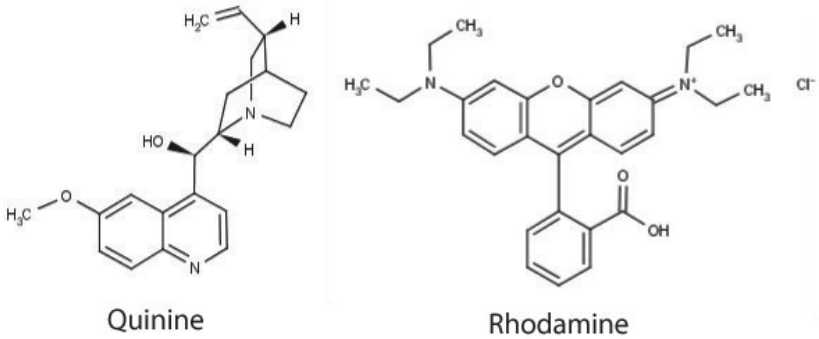


**Figure 6** - Commonly Used Fluorophores

It would not be until decades later that the mechanism by which these molecules exhibit fluorescence was explained by Alexander Jablonski. Jablonski is often credited as

the father of fluorescence spectroscopy because of his many contributions to the field. Professor Jablonski is most noted for his description of the molecular process responsible for fluorescence. The Jablonski diagram below depicts the various molecular process that lead to fluorescence.

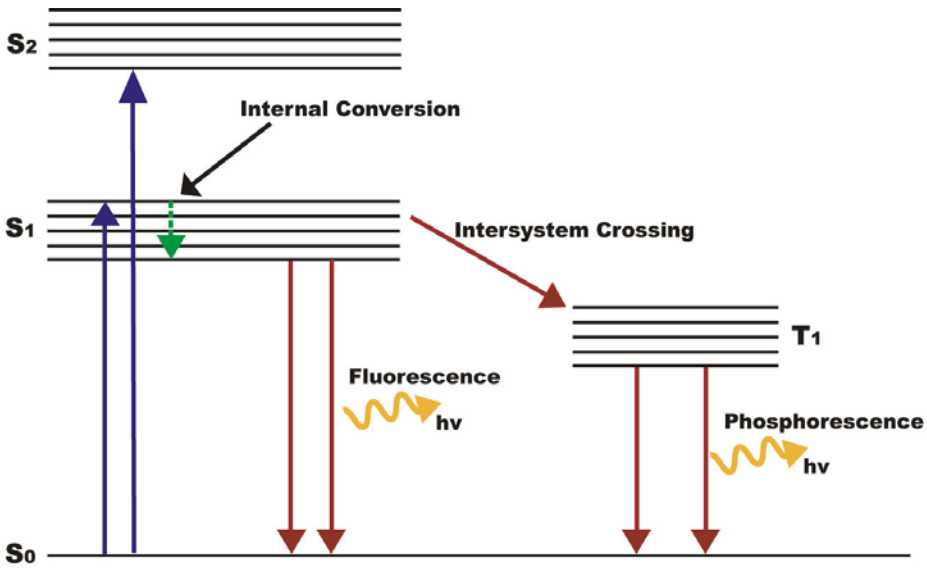


**Figure 7** - Jablonski Diagram

Figure 7 depicts the singlet state energy levels of $S_0$, $S_1$, and $S_2$. The smaller lines at each energy state represent the vibrational states. The first step in this process is absorption. Energy in the form of photons are used to excite electrons to higher energy states from the ground state. As an electron is elevated to $S_1$ or $S_2$, there are a number of pathways it can chose.

The path of least resistance is the return to $S_0$. This is true because singlet state excitation results in a pairing of opposite spins between the electrons in the excited and ground states respectively. Because the electrons are paired opposite, return to the ground

state is possible and rapid leading to the release of a photon. Any event in which photon emission occurs is termed a radiative event. The resulting photon emission, or fluorescence, occurs on the nanosecond timescale. It is possible for the photon to return to the ground state without releasing a photon. This is termed a non-radiative event.

Another possibility for photon emission is the movement of an electron from the triplet state $T_1$ to $S_0$. The release of a photon from the transition of an electron from $T_1$ to $S_0$ is termed phosphorescence. For this to occur, an excited molecule in the singlet state must move to the triplet state. This occurrence is termed intersystem crossing and is depicted in Figure 7. This is a rare event because the electrons in the triplet state share the same electron spin and this is not energetically favorable.

It is important to note that a photon is only emitted when an electron moves from the $S_1$ or $T_1$ level to the ground state. An electron may be excited to a higher energy level but fluorescence is only detectable from the transition of $S_1$ to $S_0$ [30].

During fluorescence, the excited electrons lose energy as they return to the ground state. Since energy is lost, the light emitted has a longer wavelength than the excitation source. The difference between the absorption and emission spectra is referred to as the Stoke's Shift.

Sir G.G. Stokes discovered that energy from emission is typically less than that of absorption and thus the shift in the wavelength domain can be observed [30]. The emission spectra produced is independent of the excitation wavelength used. Often a mirror image of the absorption spectra is produced in the emission spectra. This is due to the rapid relaxation of electrons in higher energy levels to the S1 state. The rapid

relaxation of excited electrons results in an emission spectra that is independent of excitation wavelength. An example of Stoke's Shift is illustrated in Figure 8. In the figure the shift between the emission and absorption spectra is apparent producing identical spectra forms.

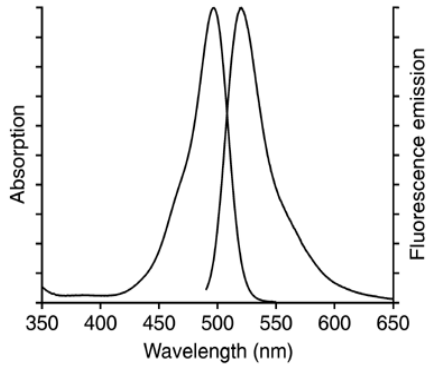


**Figure 8** - Absoption/Emission Spectra of Rhodamine

Figure 8 illustrates the longer wavelength of the emission spectra compared to the absorption spectra. By using the equation $E=h/\lambda$ it is evident that a longer wavelength corresponds to less energy. This energy must be dissipated in some other way than photon emission. It is possible for an excited electron to move down to the ground state without photon emission. This is referred to as a non-radiative event as depicted in Figure 7.

The ratio of the number of photons emitted to the sum of total photons absorbed is the quantum yield [30].Quantum yield is calculated by using Equation 5. $K_r$ and $K_{nr}$ are the rate constants of radiative and nonradiative events respectively. $K_{nr}$ only considers

non-radiative events from $S_1$ to $S_0$. Referring to Figure 7, this process is depicted. Internal relaxation events are not considered in calculating quantum yield.

$$\phi = \frac{k_r}{k_r + k_{nr}} \qquad \textbf{(5)}$$

The quantum yield of a molecule can reach near 1 if $K_{nr} << K_r$ . Such is the case for the fluorophore rhodamine. Note that the quantum yield can never reach 1 due to Stoke's loss [30]. Quantum yield is one of the most important attributes when choosing a fluorophore for a specific application. The other essential parameter to consider is the lifetime.

Lifetime is the average time a fluorophore spends in the excited state before returning to the ground state[30]. Typical fluorescence lifetimes are on the 10ns timescale. The lifetime for the fluorophore depicted in Figure 8 is defined in Equation 6.

$$\tau = \frac{1}{k_r + k_{nr}} \quad \textbf{(6)}$$

Fluorescence decay is a random process and thus Equation 6 refers to the average of time spent in the excited state. For a single exponential decay process as illustrated in Figure 17, 63% of the molecules have decayed at $t=\tau$ and the remaining 37% decay at $t>\tau$. The intrinsic lifetime is the lifetime of fluorophore in the absence of non-radiative process and is described by Equation **(7)**.

$$\tau_n = 1 / k_r \quad \textbf{(7)}$$

The intrinsic lifetime can also be calculated by combining equations 5-7, or by using the emission spectra, absorption spectra, and extinction coefficient of the fluorophore. Often the two calculations do not yield the same results. This is due to a number of factors that influence the natural lifetime such as solvent effects, refractive index change, and changes in the excited-state geometry. Lifetime measurement can be very difficult and requires the use of sensitive spectrometers with high sampling rates. The information gathered from lifetime measurement can provide a wealth of information otherwise unaccessible. By using both quantum yield and lifetime measurement a number of fluorescent probes have been developed to monitor various physical properties of the membrane bilayer.

Fluorescent probes have been employed to monitor the polarity, pH, temperature, physical phase and viscosity of membranes. Fluorescent methods provide a level of detection unavailable to mechanical methods by being able to penetrate within the core of the membrane. Current methods to monitor intermembrane viscosity provide temporal and spatial resolution that far surpass mechanical methods. With advances in imaging and probe modification, fluorescent viscosity measurement has evolved from its humble beginnings.

One of the earliest techniques of fluorescent viscosity measurement is Fluorescence Recovery After Photobleaching (FRAP)[31]. This technique determines the diffusion coefficients in the two dimensional realm of the plasma membrane. In the procedure, the membrane of interest contains a fluorescent probe with a known hydrodynamic radius. A small defined spot on the membrane is exposed to a high

intensity laser beam for a few milliseconds, and returns to a low intensity. The fluorophores in the spot area are destroyed by photobleaching. Photobleaching is the destruction of a fluorophore with high light intensities. This process then creates free radical fragments of the fluorophore in the photobleached spot. From here, surrounding dye particles then migrate into the photobleached spot and fluorescence recovery occurs. Fluorescence recovery is monitored at the spot with camera imaging until the fluorescence increase at the photobleached spot becomes stable within seconds.

This procedure assumes a Gaussian distribution of photons within the defined spot area [31]. Often the excitation beam is attenuated through a neutral density filter so as to confine the spot area and not photolyze surrounding areas. The normalized fluorescence recovery for a Gaussian intensity profile is governed by Equation 8 [31].

In Equation 8, $\tau_D$ is the 2-D characteristic diffusion time which is related to the 2-D diffusion coefficient (D) by Equation 8 [31]

$$\tau_D = \frac{\omega^2}{4D} \textbf{ (8)}$$

where ω is defined by half the width of the Gaussian profile of the focused laser beam at $e^{-2}$ times the height of the profile. The diffusion coefficient is defined by Equation 9 [31].

$$D = \frac{kT}{6\pi\eta r} \times 10^4 . \textbf{ (9)}$$

Equation 9 relates the diffusion coefficient ($D$), to Boltzmann's constant ($k$), temperature ($T$), the effective radius ($r$), and the viscosity of the medium ($\eta$). Thus, from back calculations, the viscosity of the medium can be calculated. This method was recently employed to study effects of plasma membrane viscosity on the GTPase Ras [32].

In this investigation, Green Fluorescent Protein was used tagged with Ras derivatives and transfected into COS-7 cells. The molecular probes $DiIC_{16}$, $DiIC_{18}$ are viscosity sensitive probes that were used as reference probes. These probes exhibit known changes in diffusion rates that arise from interactions with the lipids present. The diffusion of these probes were compared to that of the Ras derivatives. The COS-7 cholesterol content was either loaded or depleted and the effects on lateral diffusion of the Ras and the $DiIC_{16}$ and $DiIC_{18}$ were measured.

It was first found that acute overloading and depleting the cholesterol content significantly alter the plasma membrane cholesterol levels. The cholesterol content was confirmed by filipin staining. Secondly, altering the cholesterol levels lead to a redistribution of both the Ras and the reference probes in their respective cells.

The FRAP experiments showed that the $DiIC_{16}$ and $DiIC_{18}$ diffusion rates were unaffected by cholesterol depletion (low viscosity conditions) but lowered by acute cholesterol loading (high viscosity conditions). The lateral mobility of the Ras was lowered by both the acute loading and acute depletion of cholesterol.

FRAP has played an important role in membrane mechanics investigations. This method has some limitations in studying the effects of viscosity changes. One drawback

is the small area of analysis. The poor spatial resolution limits the ability to the study the entire membrane. A small spot size will provide a poor signal-to-noise ratio while a larger spot size lowers the resolution of the technique. A balance must be struck to meet these to criterion.

Besides issues with accuracy, this technique induces physical changes to the membrane system. High intensity laser pulses can have damaging effects that may alter local viscosity conditions. This effects may include but are not limited to, cross linking of membrane proteins, damaging the membrane through thermal stress, peripheral photobleaching outside the region of interest and free radical formation due to photolysis. It is because of these effects that the amount of error in this method is a direct function of the beam radius applied. This technique has been validated as effective means for viscosity measurement and made significant contributions to cell physiology. All fluorescent probe measurements have limitations and some of the considerations connected with FRAP can be circumvented with other methods.

Fluorescence anisotropy is another popular method for membrane investigations. When a polarized light source is used to excite a population of special fluorophores, a fraction of the resulting emission is also polarized. The measure of this polarization is described as anisotropy [3]. Polarized emission from a sample is characterized as having nonzero anisotropies. Anisotropy arises from a preferential excitation for those fluorophore who have their transition moment aligned with the electric vector of the polarized excitation wave. Therefore, the excitation process is not random. The amount of excited molecules oriented to the vector plane is instead larger than those not.

Depolarization events can occur for a variety of reasons. Rotational diffusion is one of the main causes of emission depolarization and is of special interest for viscosity investigations. A fluorophore in the excited state will rotate from the original orientation. The extent of this rotation is dependent on molecule size and shape, as well as the solvent viscosity. An excited fluorophore in a low viscosity solvent will be able to rotate quicker resulting in an almost completely depolarized emission or in other words an anisotropy of 0.

To observe this effect in solution a sample is excited with vertically polarized with respect to the z-axis. The resulting emission is then passed into a beam splitter where polarizing filters are oriented parallel and perpendicular to the excitation beam respectively. The intensity from both of these sites are then used to calculate the anisotropy. A typical apparatus is shown in Figure 9.

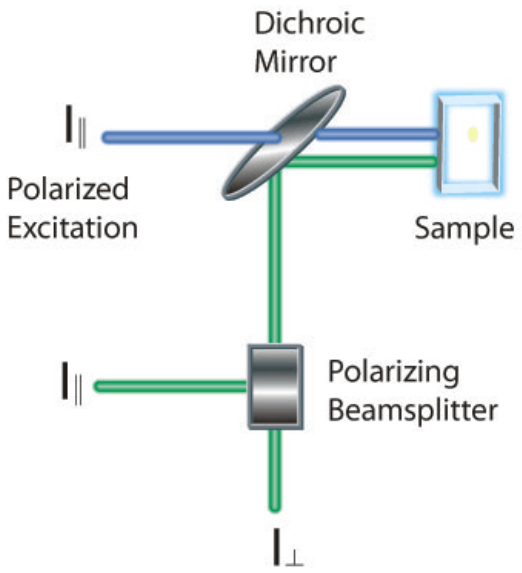


**Figure 9** - Typical Apparatus for Measuring Anisotropy

By measuring the intensity from both I‖ and I⊥ the anisotropy, which is a dimensionless measurement, can be calculated with Equation 10. The dimensionless r can be used to qualitatively measure changes in membrane viscosity.

$$r = \frac{I_{\parallel} - I_{\perp}}{I_{\parallel} + 2I_{\perp}} \quad \textbf{(10)}$$

Investigators have used the polarization sensitive qualities of the fluorescent probe DPH (1,6-diphenyl-1,3,5-hexatriene) to probe membrane viscosity in a number of ways. One recent study employed DPH to measure the ability of aniracetam to reverse the effects of both amyloid-β and aging on membrane fluidity in the brain [33]. A decrease in membrane fluidity has been reported as a result of aging [34] and amyloid-β

[35] in mouse brain. It is believed that aB plays a role in cellular calcium signaling and the impairment of oxidative stress [36]. The ability of aniracetam to restore these effects were studied on the frontal cortex and hippocampus synaptosomes using the lipophilic probe DPH.

Brain matter portions were first exposed to a β amyloid precursor. It was found that the addition of aniracetam reversed the reduction in membrane fluidity induced by aβ. Figure 10 highlights effects on the anisotropy of DPH and in turn the restoration of membrane fluidity levels to near original levels.

| Group | Frontal cortex ($r$ value) | | Hippocampus ($r$ value) | |
|---|---|---|---|---|
| | Young | Aged | Young | Aged |
| Control | $0.1830 \pm 0.0185$ | $0.1907 \pm 0.0065^{++}$ | $0.1906 \pm 0.0189$ | $0.1956 \pm 0.0074^{++}$ |
| DMSO | $0.1853 \pm 0.0149$ | $0.1911 \pm 0.0055$ | $0.1900 \pm 0.0186$ | $0.1986 \pm 0.0076$ |
| Aniracetam 0.1 | $0.1814 \pm 0.0141$ | $0.1907 \pm 0.0082$ | $0.1826 \pm 0.0145$ | $0.2003 \pm 0.0091$ |
| 1.0 | $0.1838 \pm 0.0179$ | $0.1886 \pm 0.0075$ | $0.1838 \pm 0.0203$ | $0.1978 \pm 0.0085$ |
| 2.0 | $0.1826 \pm 0.0168$ | $0.1908 \pm 0.0057$ | $0.1800 \pm 0.0136$ | $0.1860 \pm 0.0088^{*}$ |
| 4.0 | $0.1763 \pm 0.0132^{**}$ | $0.1836 \pm 0.0061^{**}$ | $0.1760 \pm 0.0163^{**}$ | $0.1836 \pm 0.0086^{**}$ |

**Figure 10** - Effects of Aniracetam on Frontal Cortex and Hippocampus Synaptosomes [33]

It was also found that with increasing concentrations of aniracetam, Ca levels were also restored to near control levels. The results of this study suggest that aniracetam may be helpful in restoring decreases in membrane viscosity experienced from the production of a β and from aging. DPH anisotropy is an effective method for qualitatively characterizing mechanical properties of the membrane. Anisotropy provides only a limited view of the physical properties. By monitoring other properties, such as

membrane water content, membrane viscosity can be better understood. Laurdan is a fluorescent probe that has been used frequently in recent membrane investigations.

The polar sensitive properties of the fluorescent probe Laurdan (6-dodecanoyl-2-dimethylaminonapthalene) have been used to investigate the physical properties of phospholipid bilayers [37]. Laurdan has been shown to be sensitive to changes in solvent polarity and temperature. This particular study investigated the abilities of Laurdan to quantify the effects of gel and crystalline phases of the lipid bilayer. As described in this chapter, the rotational rate of the fluorescent probe is a function of the local viscosity as well as temperature. The polarity sensitive attributes are believed to arise from a post-excitation orientation of the probe in respect to the surrounding polarity. The polarity conditions are dependent on the amount of water present within the membrane. By quantifying the amount of water present, estimations about local viscosity can be made. As membrane water increases, membrane viscosity decreases.

An interesting feature of this probe that a change in polarity will result in change in the spectral width of the emission [38]. To quantify these spectral shifts, Equation 11 is used to measure the generalized polarization of the probe in response to quantify changes in lipid phase domain. In this equation, $I_B$ and $I_R$ are the maximum intensities at the red and blue edges respectively, of the emission spectra. $I_B$ and $I_R$ represent the absence and presence of polar molecules respectively.

$$GP = \frac{I_B - I_R}{I_B + I_R}$$

Laurdan has shown sensitivity to mixtures of lipid compositions. Spectral shift arises from the different polarities present within the separate membranes. By measuring intensity shifts, the same governing equations used for DPH can be used to quantify changes in membrane viscosity. The dependency of anisotropy on multiple physical phenomena complicate the calculation of viscosity conditions.

Fluorescence anisotropy has made significant contributions to cell physiology and bringing a greater understanding to cellular mechanics. This technique does however have many limitations in relation to membrane viscosity studies. The rate of rotational diffusion is dependent on a variety of properties. For the membrane probe DPH, chemical composition of the membrane along with the phase state will affect the anisotropy measurement. Anisotropy measurememements are often provide weak signal and this weak signal-to-noise ratio is worsened by the polarizing filters required for signal processing. Often the signal collection time is very short due to photobleaching of the dye. Molecule size and shape, temperature, and resonance energy transfer all combine to affect the anisotropy. An exciting alternative to both fluorescence anisotropy and FRAP, is the use of molecular rotors for the investigation of membrane viscosity.

Molecular rotors belong to a family of fluorophores called Twisted Intermolecular Charge Transfer complexes or T.I.C.T. molecules [39]. These molecules possess the ability to rotate along an internal axis during excitation. This rotation is simply a non-radiative decay process that is an additional pathway for excited electrons. The amount of rotation is directly proportional to the surrounding microviscosity.

Most molecular rotors are derivatives of the p-(dialkylamino)-benzylidenemalonitrile group. Common molecular rotors are 9-(dicyanovinyl)-julolidine (DCVJ) and 9-(2-carboxy-2-cyano)vinyl julolidine (CCVJ) which are depicted in Figure 11.

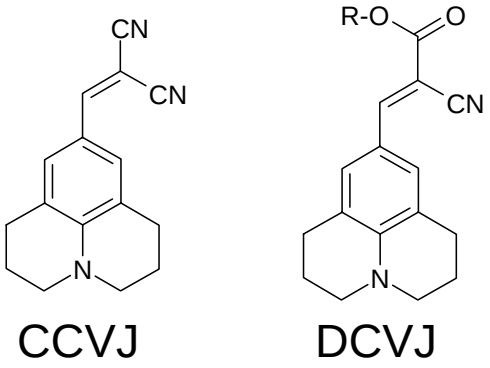


**Figure 11** - The Molecular Rotors CCVJ and DCVJ

The intrinsic rotation is a photoinduced electron transfer from the julolidine to the present nitrile group. The rotation occurs along the julolidine-vinyl bond which leads to the viscosity sensitive attribute [40]. Steric hindrance of the molecular rotor is governed by the local free volume [40]. As the local viscosity increases (low free volume) the decay process is shifted towards a higher frequency of radiative decay events. Thus fluorescence emission increases in the presence of high viscosity conditions.

TICT molecules have been investigated for more than 40 years. Z.R. Grabowsky first formulated the TICT hypothesis in 1973 [41]. Forster and Hoffman are responsible for determining the governing equation between quantum yield and local viscosity [42]. This power law relationship was proven both analytically and experimentally. The

mathematical relationship between quantum yield Φ and viscosity η is shown in the Forster-Hoffmann equation, (Equation 12), where C is a temperature dependent constant and x is a dye specific constant [43].

$$\log \Phi = C + x \log \eta \quad \textbf{(12)}$$

The viscosity sensitive abilities of molecular rotors have been proven experimentally [40]. An experimental proof of the Forster-Hoffman equation is provided in Figure 12. The graph below depicts the molecular rotor DCVJ in different mixtures of ethylene glycol and glycerol to provide different solution viscosities. The viscosity increases with the glycerol content and a corresponding increased emission intensity is observed.

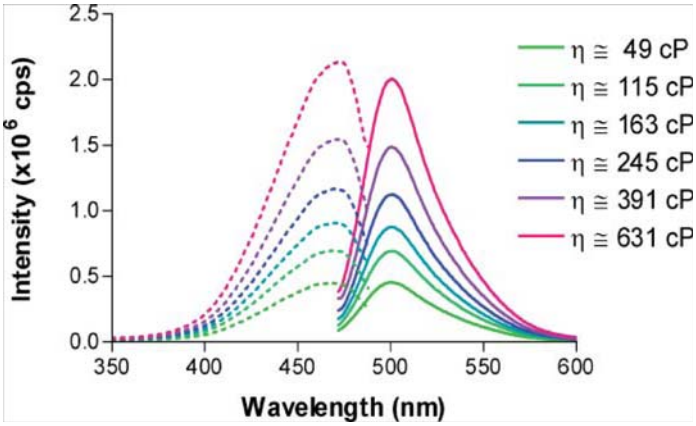


**Figure 12 -** Viscosity Dependent Emission of DCVJ [40]

Calibration of the rotor system can be made with the use of the emission spectra from samples with a known viscosity. If the absorbed light intensity $I_{ab}$ is known, the

emission intensity and quantum yield are proportionally related through $I_{em} \alpha I_{ab} \Phi$ [44]. Dye concentration needs to be considered in viscosity calculations. At low dye concentrations a linear relationship occurs between dye concentration and $I_{em}$. Determining the temperature constant C is possible yet impractical. Relative changes in viscosity can be measured by relating two emission intensities with two corresponding viscosities. Assuming constant temperature, constant absorption, and negligible background light, Equation 13 can be obtained by eliminating C [45].

$$\frac{\eta_1}{\eta_2} = \left(\frac{\Phi_1}{\Phi_2}\right)^{\frac{1}{x}} = \left(\frac{I_1}{I_2}\right)^{\frac{1}{x}} \textbf{(13)}$$

If $I_1$ is found for a solution with a known viscosity $\eta_1$, Equation 13 can be used with the experimentally gathered $I_2$ to determine the unknown viscosity $\eta_2$. Membrane viscosity measurements are highly location specific and optimal placement is required for accurate measurements.

One distinct advantage of molecular rotors over mechanical viscosity measurement is the low sample volume needed for analysis. The nanosecond response time of the photoinduced rotation allows for high speed measurement of minute changes in viscosity. With the use of fixed wavelength filters, intensity can be measured within fractions of a second.

As with all quantitative fluorescent methods, molecular rotors are associated with some challenges. Lifetime measurement would be the ideal method for estimating the quantum yield of the rotor. Currently, lifetime fluorophotometers for fluorophores with a sub nanosecond lifetime are uncommon and can be quite expensive. The most cost efficient and practical method for lifetime estimation is steady-state fluorescence.

There are a number of factors to consider when calculating viscosity from quantum yield. Unfortunately, the quantum yield of the rotor is not totally dependent on local viscosity. The rotor-containing solvent may absorb excitation or emission light, or may be scattered by small particles in turbid fluids. By measuring fluid absorption and scattering, these effects can be accounted for. Another consideration is the local dye concentration is calculating viscosity change from quantum yield. By measuring absorption of the fluid at the excitation wavelength, it is possible to account for concentration effects as well.

The emission intensity of a molecular rotor is dependent on both dye concentration and viscosity. Absorbency is a viscosity-independent function and is only dependent on dye concentration. By accounting for dye concentration, scattering and absorption, viscosity can be calculated from emission intensity by Equation 14 [46].

$$\eta = \xi I_{EM}^{\kappa} \quad \textbf{(14)}$$

In this equation, $I_{em}$ is the measured and corrected intensity, $\kappa$ is the reciprocal of x in Equation 12, and $\xi$ is a proportionality constant that depends on the above correction factors as well as on the instrument itself. $\xi$ is affected by excitation intensity, emission

collection efficiency, amplifiers, and other instrumentation affects. ξ is determined by calibration of fluids with known viscosity.

Molecular rotors have a distinct advantage over mechanical measurement devices in that they can be chemically modified to be application specific. The molecular rotors fluorescence arises from the electron transfer that occurs between the nitrogen donor and the nitrile acceptor. Thus, the rotor can be modified with targeting elements without affecting the photoinduced rotation leading to the viscosity-sensitive properties. The general form of a molecular rotor is shown in Figure 13.

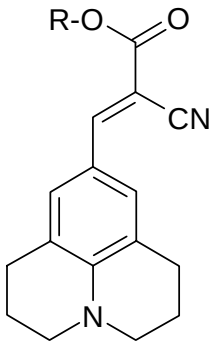


**Figure 13** - Molecular Rotor Base

Molecular rotors have been modified with a variety of functional groups for specific applications. DCVJ had been previously used in membrane viscosity investigations. While this rotor was effective in probing intermembrane viscosity, the dye also had a high binding affinity for the cell cytoplasm and tubulin structures [47]. A new fluorescent probe was designed that could exhibit a higher affinity for the cell membrane [47].

An array of CCVJ derivatives were created by attaching long-chained alcohols to the carboxylic acid portion through an ester bond. Among the group of long chained alcohols attached was a Farnesyl. Farnesyl is composed of there isoprenyl groups and isoprenyl groups have been reported to aid localizing membrane bound proteins. The reaction mechanism by which this rotor is formed is shown in Figure 15. Upon successful synthesis, the physical properties of FCVJ were compared to other molecular rotors.

FCVJ was shown to have preferential staining of the cell membrane compared to

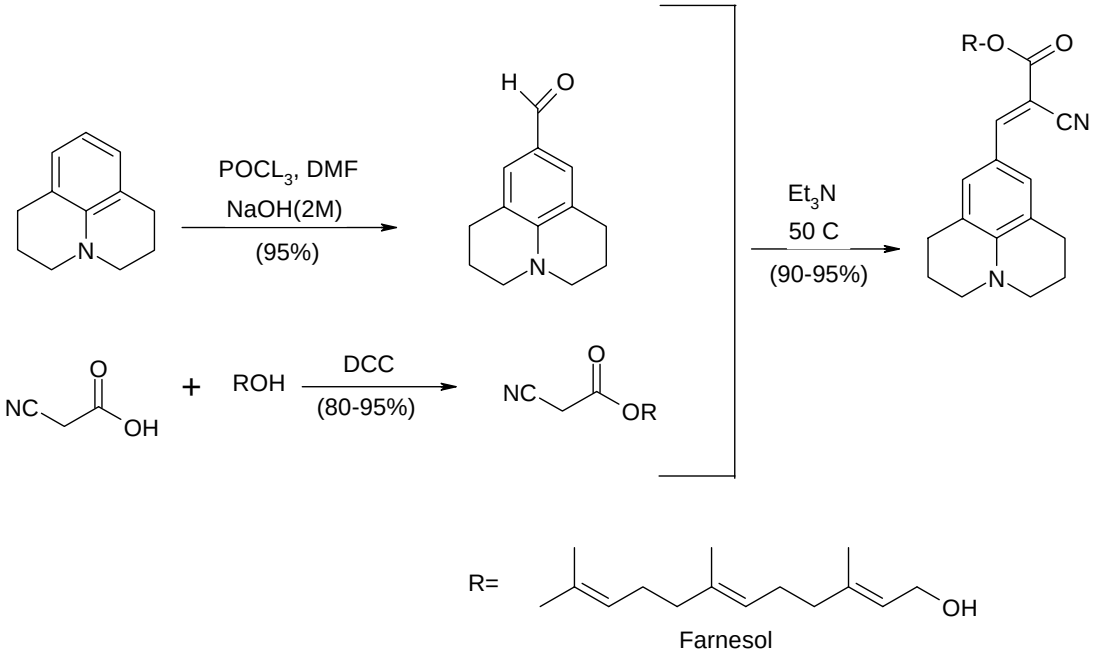


**Figure 14** - Synthesis of FCVJ [47]

that of DCVJ. A 20-fold increase in response to shear stress was reported for FCVJ compared to DCVJ. The absorption/emission spectra were close to the measured spectra for DCVJ. It was found that the FCVJ also exhibited a higher resistance to photobleaching than DCVJ.

FCVJ has demonstrated preferential placement in the membrane over both CCVJ and DCVJ. The ability of FCVJ to seek placement within the lipid bilayer arises from the bilayer affinity for the iosprenyl chain present on the farnesol. The optimal placement of this rotor within the hydrophobic core of the lipid bilayer lends itself as an excellent tool for monitoring intermembrane viscosity.

Often intermembrane viscosity measurement is affected by integral proteins, cell receptors, and ion channels. To observe the effect of a desired solvent or drug, a pure membrane modeling system should be used. Liposomes are commonly used in membrane mechanics investigations and provide a solid model to study effects on the phospholipid bilayer.

# CHAPTER 3

## Liposomes in Membrane Investigations

A liposome is simply any lipid bilayer structure that enclose an aqueous volume. phospholipids are commonly employed but not required. In mixed phospholipid systems the mix of lipids is described in terms of mole ratio. Liposomes are described in terms of the number of layers present and the total volume enclosed. The first liposomes formed in a laboratory were multilamellar vesicles (MLVs) [48]. These were concentric lipid layers that from shell shape structure. If the lipid solution is sonicated, single unilamellar vesicles (SUVs) are formed. These vesicles have a diameter in the range of 25-50 nm. There are a number of limitations for both of these vesicle systems. Large unilamellar vesicles are the third type of vesicles that can be formed. LUVs typically range from 100-500 nm in diameter. The three types of liposomes are depicted in Figure 15.

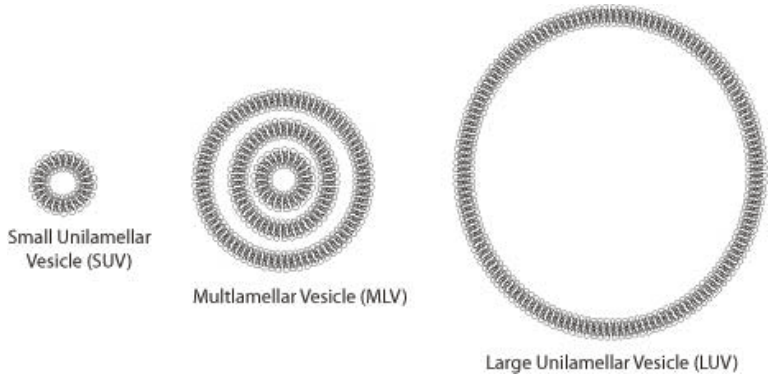


**Figure 15** - Different Liposome Sizes

There are a number of ways liposomes can be produced. The lipid combination is dependent on investigator preference along with application specifics. Both the charge and lipid composition determine the size of the liposome. Common methods include

lipid film hydration/sonication and electroformation. A common lipid film hydration protocol consists of dehydrating a solution of lipid dissolved in chloroform under a nitrogen stream in a glass tube. The tube is then filled with the desired amount of formation solution and gently vortexed to form MLVs. If SUVs are desired, the solution is sonicated.

An alternative to this method is the electroformation process. In a typical protocol, the lipid/chloroform solution is deposited on parallel platinum wires. A uniform AC electric field is then applied to the wires in the presence of the formation solution. The formation is monitored under light/fluorescence microscopy and the AC field is stopped when the desired diameter is reached. Once again, the signal strength and duration of the field are dependent on the lipid used. The electroformation process has been shown to produce more LUVs with fewer defects compared to the hydration/sonication method [49].

The pure lipid bilayer structure have made liposomes an attractive model for a variety of applications including, drug delivery systems [50], and miniature bioreactors [51]. The most popular use for liposomes has been the use of liposomes as a model to investigate mechanical properties of the cell, including membrane viscosity [52].

# CHAPTER 4

## Experiment Design and Rationale

It is evident that changes in membrane viscosity are of great significance to understanding cellular responses. As discussed in Chapter 1, the mechanical methods employed to measure intermembrane viscosity are limited and provide poor temporal and spacial resolution. Logically, fluorescent probes lend themselves to be the most reasonable method for investigation of microviscosity within the membrane. With these facts in mind, the choice was made to use the molecular rotor FCVJ to measure membrane viscosity changes in a liposomal system.

Liposomes formed from 1,2-Dilauroyl-sn-Glycero-3-Phosphocholine (DLPC) were chosen because their size is similar to the human cell diameter (7-15 um). An electroformation protocol was used to produce large unilamellar vesicles. To measure intermembrane viscosity change, the rotor must be placed within the hydrophobic core of the membrane. Chapter 2 highlights the farnesol group present on the rotor. The affinity of the membrane for the isoprenyl chain along with the hydrophobicity of the dye forces the rotor into the hydrophobic core of the membrane during formation.

After the liposome formation is complete, the rotor will be in the core of the membrane. To check this fluorescence spectroscopy is used to image the vesicles. Upon confirmation of rotor placement, the liposomes can be used in viscosity altering experiments.

The first set of experiments are to investigate the effects of alcohols and organic solvents on the membrane. Short chained alcohols were chosen because of the extensive

evidence to prove that alcohols reduce membrane viscosity [53]. The degree by which the viscosity is a direct function of carbon chain length. Traube's rule states that with each additional methyl group, the potential energy increases three fold, which results in a linear trend in the effect on membrane viscosity [53].

Continuing with trying to achieve this desired reduction in viscosity the organic solvent Dimethyl Sulfoxide was chosen in the investigation. Evidence suggests that DMSO induces the formation of water pores within the membrane leading to a reduction in viscosity [54]. The other organic solvent tested was cyclohexane. The hydrophobic nature of this solvent made the study of the effects on membrane viscosity quite appealing.

To observe increases in membrane viscosity, liposomes were formed with cholesterol. In the membrane, cholesterol acts as a spacer between the polar heads in the membrane [2]. The resulting effect is an increase in membrane viscosity. Cholesterol was chosen for its well documented effects on membrane viscosity as well as the great importance in many biological processes. Due to the hydrophobic nature of sterols, the cholesterol must be mixed with the lipids prior to the formation step.

Many pharmaceuticals today function by altering the mechanical properties of the membrane. With this in mind, the effects of two widely used pharmaceuticals, nimesulide and tamoxifen, on membrane viscosity were investigated. Both are hydrophobic and must be introduced to the lipid prior to electroformation.

# CHAPTER 5

# Materials and Methods

## 5.1 Liposome Electroformation Protocol

An electroformation process was chosen to produce single unilamellar vesicles (SUV's). The electroformation has shown to produce more SUV's with less defects compared to the more classical lipid film/hydration protocol [49]. The liposome electroformation took place in a chamber as illustrated in Figure 16.


**Figure 16** - Liposome Electroformation Chamber

### 5.1.1 Chamber cleaning

- Chamber brushed with alconox and water
- Rinse with water/methanol 1:1
- Sonicate the chamber in Alconox/Water/Methanol 1:1:1 for 15 minutes
- Rinse with methanol/water 1:1
- Sonicate the chamber in Water/Methanol 1:1 for 15 minutes
- Rinse with methanol/water 1:1
- Rinse with deionized water

### 5.1.2 Syringe Cleaning

- Prepare 2 ml glass syringe by rinsing with chloroform 10-15 times

- Allow to air dry

5.1.3 Lipid Preparation

- Add 10 ul of 2.5 mM FCVJ to 200 ul DLPC(Avanti) in a glass vial
- Gently vortex
- Withdraw lipid/rotor solution into glass syringe
- Deposit lipid/rotor solution onto platinum wires in formation chamber in small dots until the syringe is empty

5.1.4 Stock Sucrose Solution Preparation

- Prepare 500 ml of 250 mM sucrose (Sigma) solution in ddH20

5.1.5 Chamber Preparation

- Place chamber and sucrose solution under vacuum for 15 minutes
- Remove the chamber, keep sucrose under vacuum
- Adhere 2 glass slides to the chamber with vacuum grease (Dow) making sure not to contaminate the electrodes with the grease
- Place the chamber in the metal clamp
- Remove sucrose solution from vacuum
- Fill 2ml plastic syringe with sucrose solution
- Fill chamber with sucrose solution $\approx$2 mL

5.1.6 Electroformation

- Place the chamber on the microscope stage
- Attach alligator clips from function generator to platinum wires

- Turn on the function generator and set the frequency to 10 Hz
- Set amplitude to 1 V
- Feed signal for 10 minutes
- Lower frequency to 1 Hz
- Feed signal for 7 minutes
- Turn off the function generator
- Extract the liposome suspension with clean 2 mL syringe
- Deposit liposome suspension into microcentrifuge tube

## 5.2 Experiment Setup - Alcohols and Organic solvents

### 5.2.1 Control Group

- Pipette into 950 μL of stock sucrose solution in a 1.5 ml plastic microcuvette
- Pipette 50 μL of liposome suspension into the sucrose solution
- Cap the cuvette
- Gently vortex
- Repeat for 10 control samples

### 5.2.2 Experimental Group

- Prepare 2% (v/v) methanol(Sigma)/stock sucrose solution
- Pipette 950 μL of methanol/sucrose solution into 1.5 ml microcuvette
- Pipette 50 μL of liposome suspension into the methanol/sucrose
- Cap the cuvette
- Gently vortex
- Repeat for 10 experimental samples
- Repeat for ethanol(Sigma) and propanol(Sigma)

### 5.2.3 Steady-State Fluorescent Spectroscopy

- Place the control and experimental groups in a temperature controlled turret (Quantum Northwest - TC 425)
- Alternate samples between control and experimental to account for time effects

- Set temperature turret to 30ºC
- Place turret into fluorospectrometer (Jobin-Yvon FluoroMax-3)
- Excite at 460 nm
- Record emission spectra from 470-600 nm
- Repeat steady-state fluorescence spectroscopy procedure
- Repeat entire procedure for desired alcohol or concentration

## 5.3 Experiment Setup - Organic Solvents

### 5.3.1 DMSO Group

- Prepare 10 control samples as previously described
- Prepare a 30 mol% DMSO(Sigma)/250 mM sucrose solution
- Pipette 950 μL of DMSO(Sigma)/250 mM sucrose into a 1.5 mL microcuvette
- Pipette 50 μL of liposome suspension into the cuvette
- Cap the cuvette
- Gently vortex
- Repeat steady-state fluorescence spectroscopy protocol

### 5.3.2 Cyclohexane Group

- Prepare 10 control samples as previously described
- Prepare a 2% (v/v) cyclohexane (Sigma)/ 250 mM sucrose solution
- Pipette 950 μL of cyclohexane/sucrose into a 1.5 mL microcuvette
- Pipette 50 μL of liposome suspension into the cuvette
- Cap the cuvette

- Gently vortex
- Repeat steady-state fluorescence spectroscopy protocol

## 5.4 Experiment Setup - Pharmaceutical Group

### 5.4.1 Nimesulide Liposomes

- Prepare 10 control samples as previously described
- Add 10 µl 10mM nimesulide (Sigma), dissolved in methanol (Sigma), to 180 µl DLPC
- Pipette 10 µL 2.5 mM FCVJ into DLPC/Nimesulide
- Repeat Electroformation process
- Prepare 10 samples of 50 µl nimesulide liposomes in 950 µl sucrose (250 mM)
- Repeat steady-state fluorescence spectroscopy protocol

### 5.4.2 Tamoxifen Liposomes

- Prepare 10 control samples as described earlier
- Add 20 ul of .05 mol% Tamoxifen (Sigma)/Chloroform (Sigma) to 180 ul DLPC (Avanti) into glass vial
- Pipette 10 ul of 2.5 mM FCVJ into Tamoxifen/Chloroform/DLPC
- Gently rotate while drying with nitrogen stream
- Evaporate under vacuum for 10 hours
- Add 10 ul of stock sucrose solution for 10 minutes
- Add 2 ml of stock sucrose solution and incubate at 37$^{o}$C for 4 hours
- Sonicate in water bath for 10 minutes

- Prepare 10 samples of 50 µl tamoxifen liposomes in 950 ul sucrose (250 mM)
- Repeat steady-state fluorescence spectroscopy protocol
- Repeat tamoxifen liposome protocol for .1, .5, 1, 2, 4, 7.5, and 15 mol%

## 5.5 Data Analysis

- Graph Pad Prism was used to perform statistical analysis
- The peak intensity is taken from each sample
- The peaks are then averaged for the group
- The control and treatment mean intensities are then plotted along with the standard deviation
- In a single variable experiment, the groups are checked for statistical significance using the student's T-test
- In multiple variable experiments, the ANOVA is used for statistical analysis with a one-tailed post test.

# CHAPTER 6

## Results and Discussions

The first step in the procedure protocol is to verify the placement of the rotor within the lipid bilayer. This is done with fluorescence microscopy. Figure 17 highlights the rotor placement within the membrane. The rotor is successfully integrated within the bilayer as seen in the image.

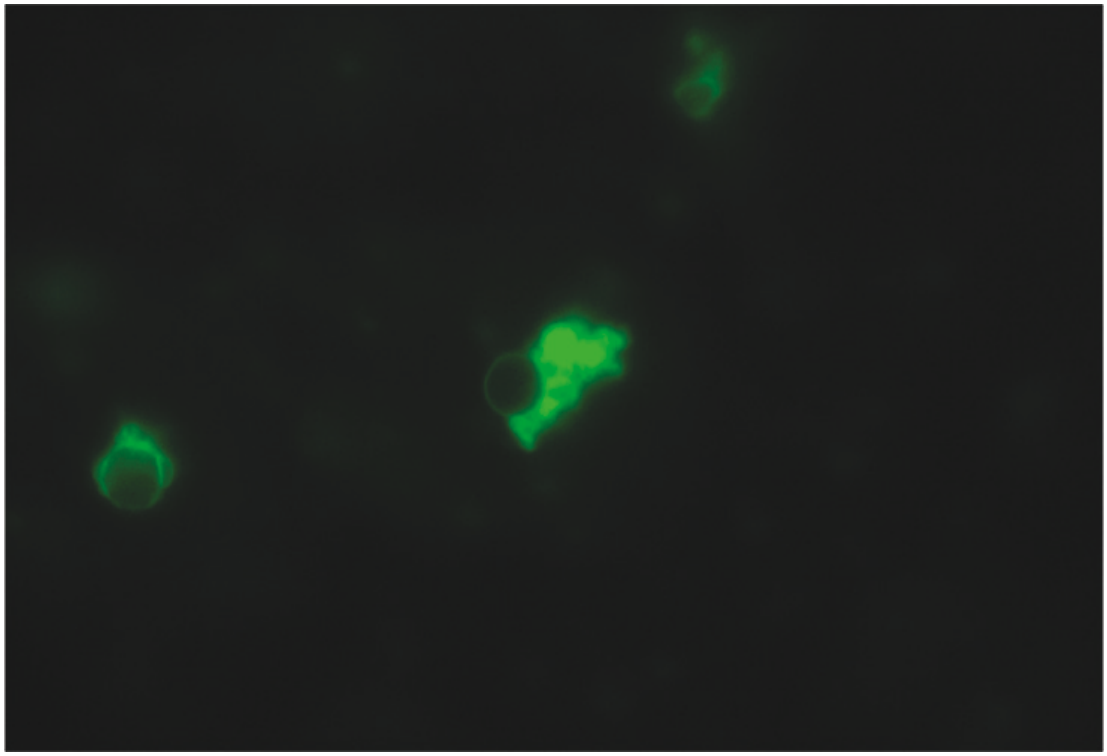

**Figure 17** - Liposomes with FCVJ Incorporated into the Membrane Viewed at 10x

The first set of experiments investigate the effects of alcohol on membrane viscosity. The effects of alcohols on the membrane are well documented and have all shown to reduce membrane viscosity [55] . As the short chain alcohol enters the

membrane, the nonpolar chain intercalates with the headgroup of the phospholipid leading to an increase in disorder which is responsible for the decrease in viscosity [53].

In Figure 18 the 2% (v/v) Methanol/Sucrose solution produces no significant effects (<1%) on the membrane viscosity. This is not surprising given the low interfacial energy arising from the single carbon bond as well as the small concentration used.

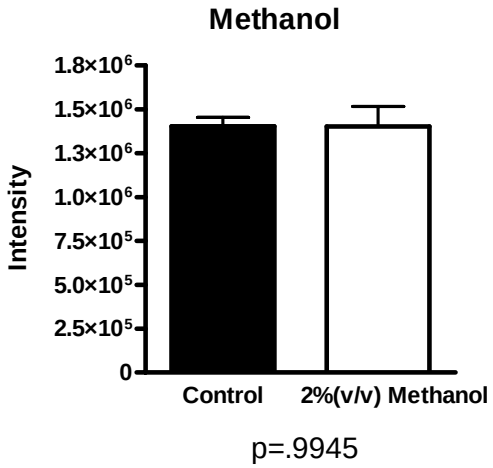


**Figure 18** - Methanol Effects

The next experiment set was to investigate the effects of ethanol on the membrane. A more significant effect was expected and as Figure 19 illustrates, the reduction of 8.7% is more pronounced in the ethanol group. As expected, the addition of a single methyl group on the straight chained alcohol produced a larger decrease in the rotor intensity. The corresponding decrease in intensity is relative to the decrease in viscosity induced by the alcohol.

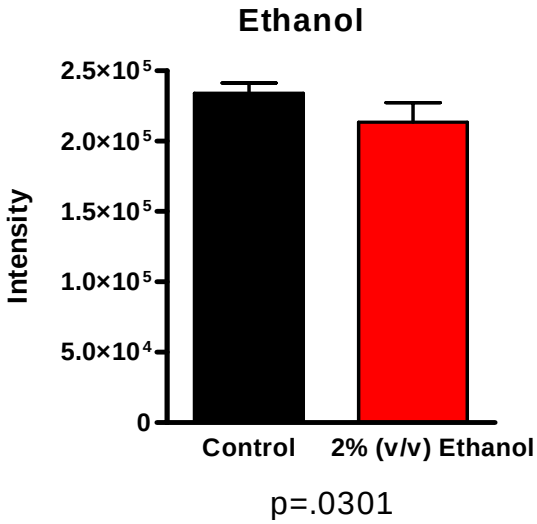


**Figure 19** - Ethanol Experiment Results, N=10

Continuing the trend, propanol was the next alcohol tested. As expected, Figure 20 shows a decrease in intensity of 13.8%. The effect was more profound than the previous two alcohols as predicted.

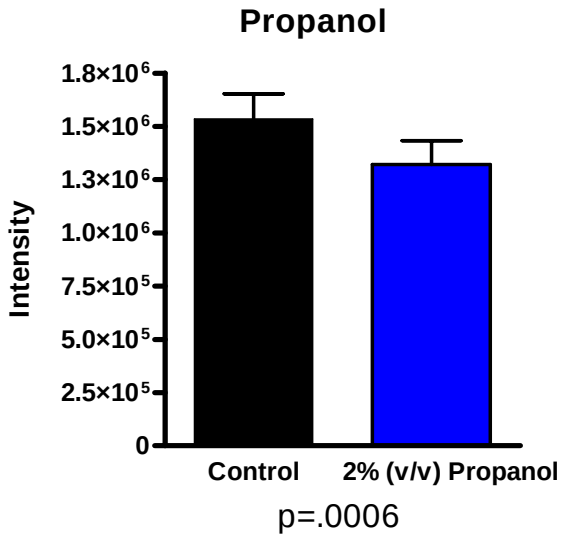


**Figure 20** - Propanol Experiment Results, N=10

This occurrence follows Traub's Rule which states that with the addition of a single methyl group on an alcohol, the effect on the membrane increases by approximately 33%. Figure 21 illustrates the relationship between carbon chain length and decrease in viscosity.

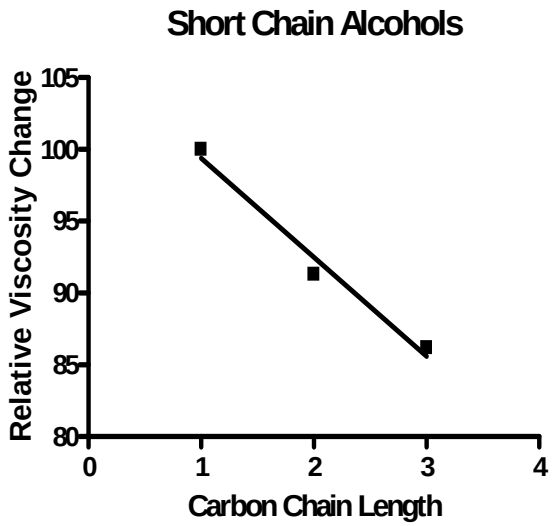


**Figure 21** - Carbon Chain Length vs. Relative Viscosity Change ($R^2$=.9779)

As Figure 21 confirms, the longer the carbon chain, the more profound effect on the membrane viscosity. To test the resolution of the FCVJ, a concentration gradient experiment was designed using propanol to determine the resolution. Propanol was chosen for having the most profound effect, a 13.8% reduction, on membrane viscosity as found from the alcohol experiments. In this experiment, concentrations of 2% (v/v), 1% (v/v), 0.5% (v/v), and 0% (control) were all tested. All of these liposomes were from the

same batch to account for concentration effects. Figure 22 illustrates the results of our experiment.

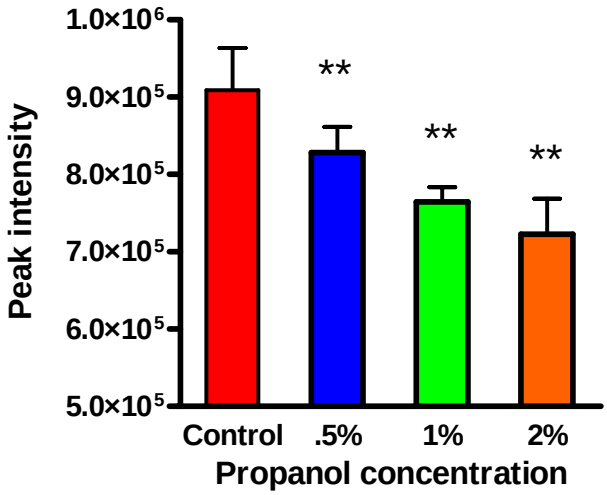


**: ANOVA/Dunnett's: p<0.01 vs. control

**Figure 22** - Propanol Dose Response, N=10

From this experiment it is shown that the method presented is sensitive to even minute changes in viscosity. Figure 23 demonstrates the high resolution and sensitivity to minute changes in viscosity. The linear relationship between concentration and relative viscosity change is shown in Figure 23.

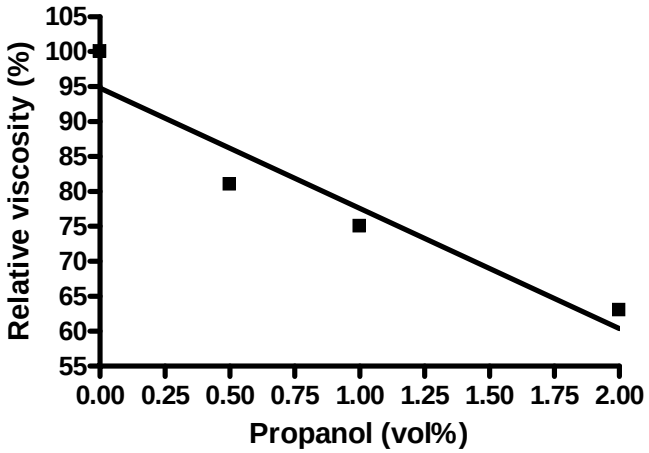


**Figure 23** - Relative Viscosity vs. Propanol Concentration ($R^2$=.9054)

The data presented is in agreement with numerous publications citing the effects of short chain alcohols on the membrane. Our data demonstrates the high sensitivity to concentration as well as the linear relationship exhibited between carbon chain length and effects on viscosity. The effects of organic solvents on the membrane were the next area of investigation.

DMSO has been shown to spur the formation of water pores within the membrane [54]. The amphiphilic nature of this molecule draws the DMSO molecule to the lipid-water interface of the membrane. This nature draws the molecule to occupy a space under the polar heads of the membrane. This action in turn increases spacing within the membrane leading to water pores, and ultimately an increase in permeability [54]. This same action also causes the membrane to become more pliable which would one would

ration would equal a decrease in viscosity. The next set of experiments investigates this theory.

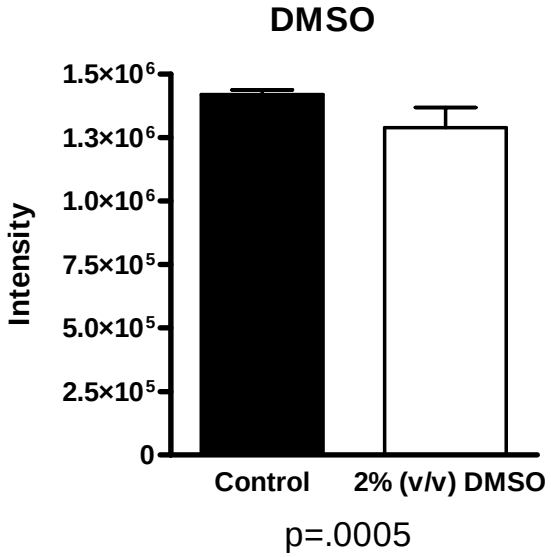


**Figure 24** - DMSO Experiment Results, N=10

Figure 24 illustrates the 9.2% reduction in intensity compared to control. This suggests that the addition of DMSO to solution produces a reduction in membrane viscosity which follows our hypothesis. The other organic solvent tested was cyclohexane. One would assume the ring structure of cylcohexane would make it nearly impossible to dissolve into solution. This is the case for most concentrations, however very small amounts can be successfully dissolved into solution. The mechanism by which this happens is a reorientation of the water bonds in solution to surround the cyclohexane molecules [2]. The resulting formation is a water cage. It is by this mechanism in

combination with vapor pressure by which the dissolution of cyclohexane was possible. Figure 25 illustrates the results of our experiments.

From the results, it is evident that the cyclohexane affected membrane viscosity in

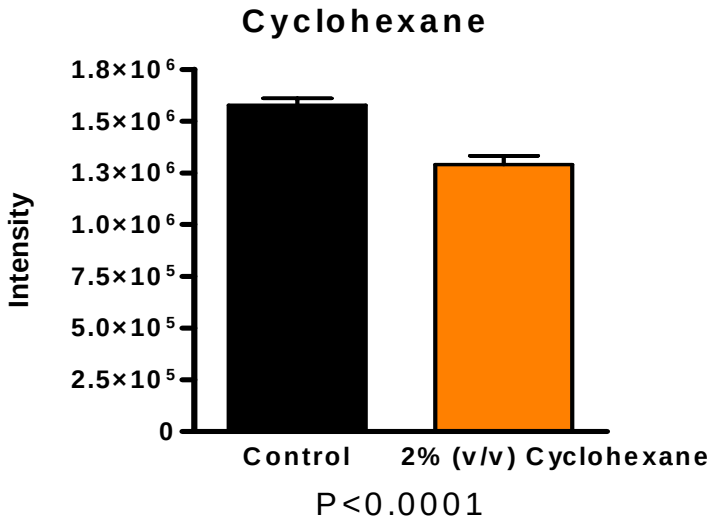


**Figure 25** - Cyclohexane Experiment Results, N=10

a profound manner. The 18.2% reduction in viscosity is both drastic and statistically significant. It is believed that the amount of cyclohexane used (2% v/v) was small enough to successfully dissolve into the stock sucrose solution.

As discussed in Chapter 1, cholesterol plays a central role in controlling cellular processes through the action of the membrane. Cholesterol acts as a separator in the membrane leading to an increase in viscosity [2]. In this experiment set, liposomes were formed with a 30 mol% cholesterol/lipid mixture. Liposomes with no cholesterol in the membrane were used as the control set.

Along with cholesterol, the arthritis drug nimesulide must be given special consideration during the formation process. Nimesulide is a cyclooxygenase (COX-2)

inhibitor commonly diagnosed to prevent inflammation as a result of arthritis. The COX-2 inhibitor works by interfering with prostaglandin synthesis and as a result curbs inflammation. Nimesulide has been shown to cause gastric side effects and the cause of this phenomenon is not well understood [56]. Upon contact with cells, the nimesulide is believed to bury deep within the hydrophobic core of the membrane [56]. Due to this hydrophobicity, the nimesulide needs to be introduced prior to the electroformation

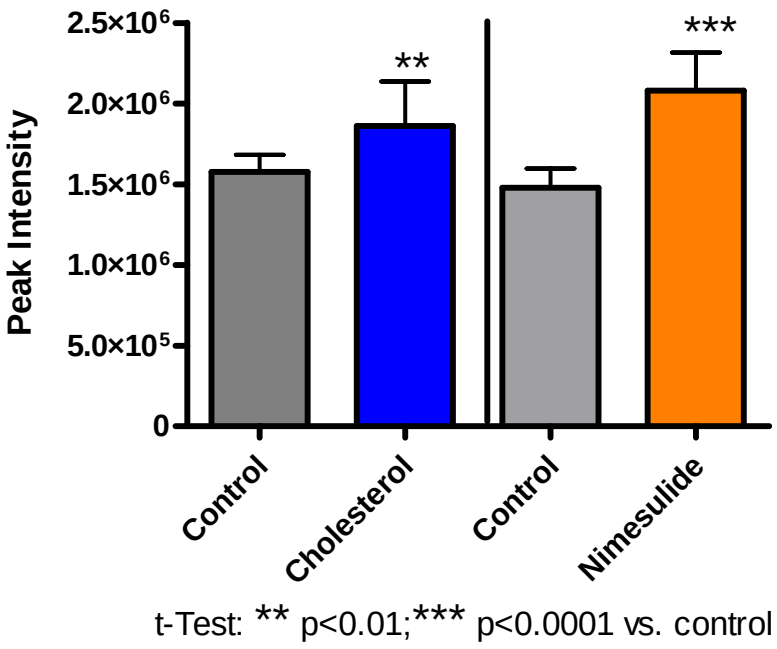


**Figure 26** - Nimesulide and Cholesterol Experiment Results, N=10

process. Figure 26 highlights the experiment results from both the cholesterol and nimesulide experiments.

The results for both the cholesterol and nimesulide show an increase in viscosity compared to control. The cholesterol group reports an increase of 18%, while the

nimesulide shows a 41% increase in intensity. This follows the hypothesis that because of their hydrophobic nature and increased packing within the core, the membrane viscosity will be increased.

The most complicated investigation in this project was the effects of tamoxifen on membrane fluidity. Tamoxifen is an anti-cancer drug that has been in popular use since the 1970's. Tamoxifen acts in a number of ways on the mechanical properties of cells including both beneficial and harmful side effects. One of the unique properties of this drug is that it acts like estrogen in some tissues while the opposite effect is observed in other tissues. Tamoxifen has been found to prevent free-radical oxidation in both biological membranes and liposomes [57]. It is believed this ability arises from the sterol groups on the tamoxifen molecularly modulating the fatty acid side-chains on the phospholipid tails [58]. However, membranes have been observed to become resistant to the drug's membrane altering properties over time. This mechanism is unknown and it is believed that this is a result of a cellular mechanical modulation of the membrane. Further investigation of the effects on membrane viscosity may help answer some of these questions.

To date, there have been conflicting reports on tamoxifen's effect on membrane viscosity. Previous studies on membranes and model systems found that tamoxifen caused a disordering effect in the bilayer, leading to an increase in chain flexibility [59-61]. The majority of studies have reported the stabilizing effects of tamoxifen on the bilayer leading to an increase in membrane viscosity. One article found that membrane viscosity of DPPC liposomes was increased at low concentrations (1 mol%) and

decreased at higher concentrations (30 mol%) [62]. Some literature suggests an increase in viscosity while one paper reported that with small concentrations, viscosity decreases,

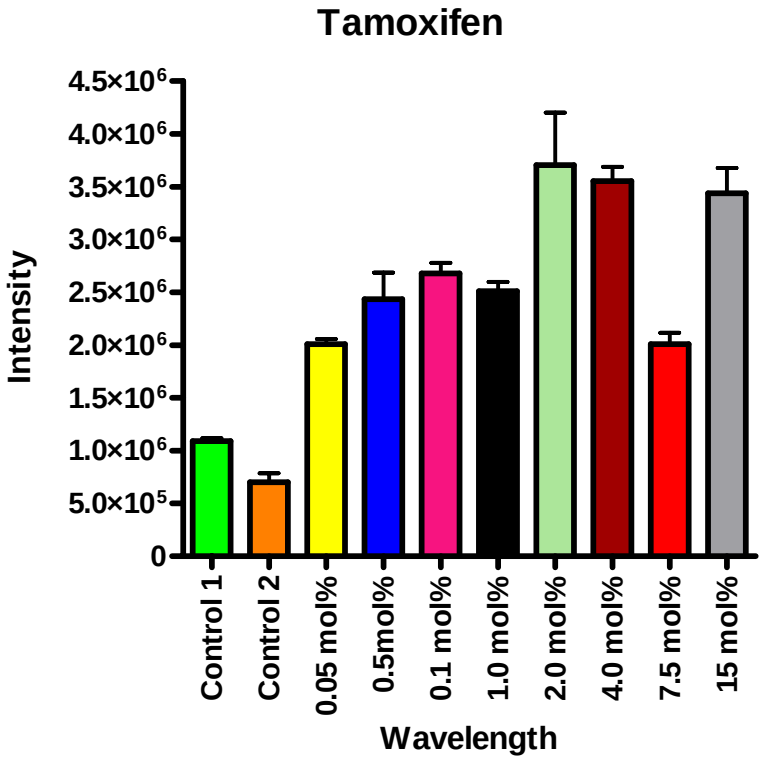


**Figure 27** - Tamoxifen Experiment Results, N=10

then increases as concentration passes 2 mol%. With these reported findings, this seemed like an excellent experiment to investigate the sensitivity of our viscosity-sensitive rotor. As stated earlier, tamoxifen is exhibits high hydrophobicity. This requires the addition of the drug to the lipid prior to the electroformation process in a similar manner to the cholesterol and nimesulide experiments. It was found that the extreme hydrophobic nature of this drug caused the lipid to cling to the platinum wires making evacuation of the chamber nearly impossible. To remedy this, an alternate liposome formation protocol

was utilized. An adapted lipid film formation protocol was used in place of the electroformation protocol. One distinct advantage of this method is a tighter control of dye concentration. The results of the experiment are shown in Figure 28.

Figure 28 shows that a general trend towards an intensity increase is observed compared to control in all groups. One important note is that two independent control groups were used in this study. The lack of a defined linear trend may have to do with solution effects as the concentration increased. There were significant solubility issues once the 2.0 mol% threshold was passed. Because of these solubility issues, turbidity effects are more pronounced in the concentrations over 2 mol%. Also upon investigation, it was found that tamoxifen exhibited autofluorescence which may have impacted our results. Figure 28 highlights these results.

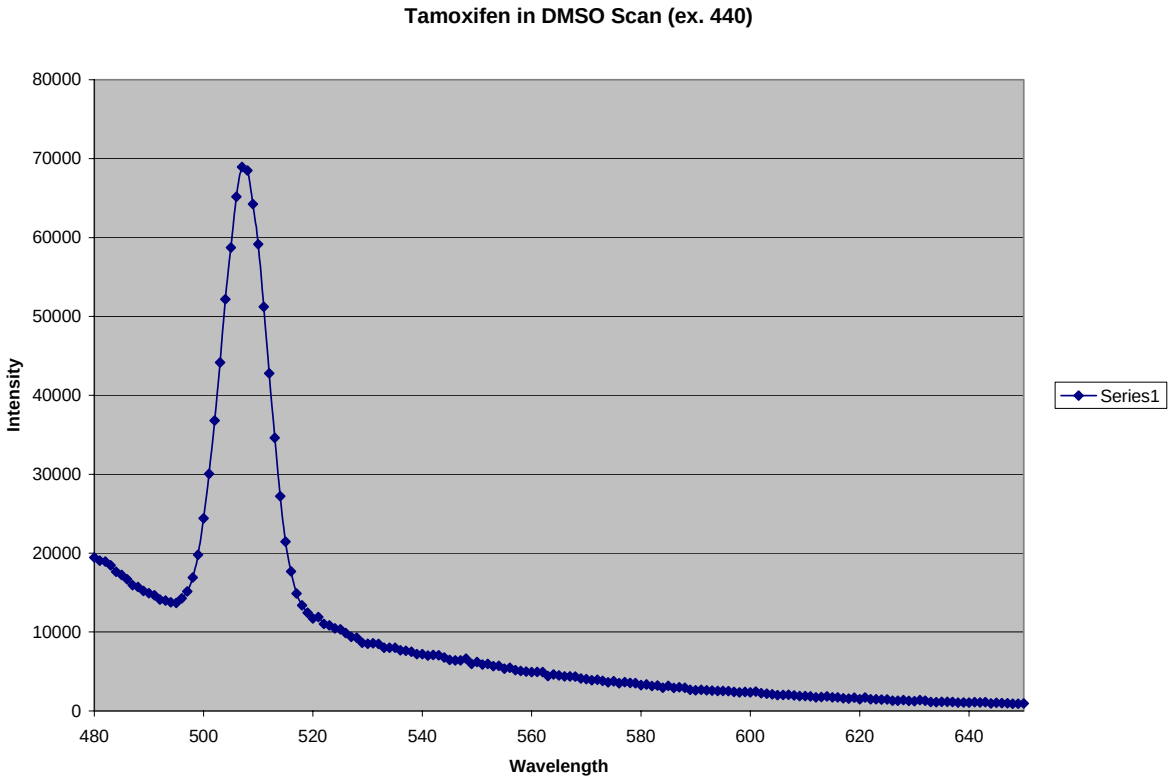


**Figure 28** - Autofluorescence Scan for Tamoxifen in DMSO

The results of the tamoxifen scan show a fluorescence peak occurring at 507 nm. It is reasonable to assume that the fluorescent properties of this drug affected the spectrofluorometer readings and in turn our viscosity calculations in a concentration dependent manner.

# CHAPTER 7

## Conclusion and Future Research Suggestions

Our results conclusively show that the molecular rotor FCVJ was successfully integrated into the hydrophobic core of the liposomal membrane. Upon integration into the core, the rotor showed sensitivity to changes in local viscosity through multiple ways. The statistical significance obtained for each group is conclusive evidence that this is an effective system for monitoring the effects of membrane altering agents.

As in all experimental methods, this system does have limitations. One factor that is hard to control is the effect of concentration on the intensity. This effect was minimized by using liposomes from the same batch in both the alcohol and short chain alcohol experiments. Future work will include the use of ratiometric dye systems that account for the concentration effects while still providing a viscosity sensitive molecular probe.

In this system a viscosity insensitive dye is covalently linked to a viscosity sensitive molecular rotor [40] . By choosing the appropriate linker length, the distance between the two dyes would be in the proximity to the Forster distance. By choosing two dyes with spectral overlap, resonance energy transfer will take place. This provides a reference concentration in order to account for concentration effects [40].

The reference dye, or viscosity insensitive portion, is a coumarin linked to the molecular rotor portion. Figure 29 depicts the ratiometric dye system to be used in future membrane viscosity investigations.

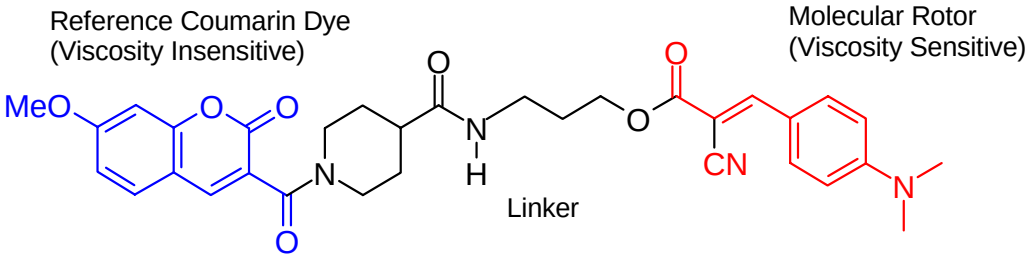


**Figure 29** - Ratiometric Dye System to be Used in Future Investigations [40]

The ratiometric dye system provides a unique tool to monitor viscosity change while accounting for concentration effects. The first step of future research is to confirm the ability to detect viscosity changes within the liposomal membrane.

The next logical step in this research is to move to an actual mammalian membrane system. For this purpose, red blood cell ghosts will be used. By lysing erythrocytes, the intracellular components are removed and the intact plasma membrane remains. This membrane retains the integral proteins and receptors within the membrane. It is unknown how the ratiometric dye will congregate in the membrane but it is believed that the dye will migrate towards the polar heads within the membrane [40].

The impact of this research is far reaching and will be of great importance to researchers in both the medical and cellular mechanics fields. The ability to monitor changes in membrane viscosity will allow for the ability to identify cells in disease states, abnormalities in membrane composition, and give clinicians another tool in treating and diagnosing disease.

# REFERENCES


[1] White FM. Fluid mechanics. 5th ed. Boston: McGraw-Hill; 2003. Pgs 866

[2] Yeagle P. The membranes of cells. 2nd ed. San Diego: Academic Press; 1993. Pgs 349

[3] Shinitzky M. Physiology of membrane fluidity. Boca Raton, Fla: CRC Press; 1984.

[4] Singer SJ, Nicolson GL. The fluid mosaic model of the structure of cell membranes. Science 1972 Feb 18;175(23):720-31.

[5] Eze MO. Membrane fluidity, reactive oxygen species, and cell-mediated immunity: implications in nutrition and disease. Med Hypotheses 1992 Apr;37(4):220-4.

[6] Heron DS, Shinitzky M, Hershkowitz M, Samuel D. Lipid fluidity markedly modulates the binding of serotonin to mouse brain membranes. Proc Natl Acad Sci U S A 1980 Dec;77(12):7463-7.

[7] Koike T, Ishida G, Taniguchi M, Higaki K, Ayaki Y, Saito M, Sakakihara Y, Iwamori M, Ohno K. Decreased membrane fluidity and unsaturated fatty acids in Niemann-Pick disease type C fibroblasts. Biochim Biophys Acta 1998 Apr 28;1406(3):327-35.

[8] Zakim D, Kavecansky J, Scarlata S. Are membrane enzymes regulated by the viscosity of the membrane environment? Biochemistry 1992 Nov 24;31(46):11589-94.

[9] Gleason MM, Medow MS, Tulenko TN. Excess membrane cholesterol alters calcium movements, cytosolic calcium levels, and membrane fluidity in arterial smooth muscle cells. Circ Res 1991 Jul;69(1):216-27.

[10] Nadiv O, Shinitzky M, Manu H, Hecht D, Roberts CT, Jr., LeRoith D, Zick Y. Elevated protein tyrosine phosphatase activity and increased membrane viscosity are associated with impaired activation of the insulin receptor kinase in old rats. Biochem J 1994 Mar 1;298 ( Pt 2):443-50.

[11] Deliconstantinos G, Villiotou V, Stavrides JC. Modulation of particulate nitric oxide synthase activity and peroxynitrite synthesis in cholesterol enriched endothelial cell membranes. Biochem Pharmacol 1995 May 26;49(11):1589-600.

[12] Osterode W, Holler C, Ulberth F. Nutritional antioxidants, red cell membrane fluidity and blood viscosity in type 1 (insulin dependent) diabetes mellitus. Diabet Med 1996 Dec;13(12):1044-50.

[13] Shiraishi K, Matsuzaki S, Ishida H, Nakazawa H. Impaired erythrocyte deformability and membrane fluidity in alcoholic liver disease: participation in disturbed hepatic microcirculation. Alcohol Alcohol Suppl 1993;1A:59-64.

[14] Maczek C, Bock G, Jurgens G, Schonitzer D, Dietrich H, Wick G. Environmental influence on age-related changes of human lymphocyte membrane viscosity using severe combined immunodeficiency mice as an in vivo model. Exp Gerontol 1998 Aug;33(5):485-98.

[15] Zubenko GS, Kopp U, Seto T, Firestone LL. Platelet membrane fluidity individuals at risk for Alzheimer's disease: a comparison of results from fluorescence spectroscopy and electron spin resonance spectroscopy. Psychopharmacology (Berl) 1999 Jul;145(2):175-80.

[16] Tanford C. The hydrophobic effect: formation of micelles and biological membranes. 2nd ed. New York: Wiley; 1980. Pgs 233

[17] Yeagle PL. Modulation of membrane function by cholesterol. Biochimie 1991 Oct;73(10):1303-10.

[18] McIntosh TJ. The effect of cholesterol on the structure of phosphatidylcholine bilayers. Biochim Biophys Acta 1978 Oct 19;513(1):43-58.

[19] Demel RA, Bruckdorfer KR, van Deenen LL. The effect of sterol structure on the permeability of liposomes to glucose, glycerol and Rb +. Biochim Biophys Acta 1972 Jan 17;255(1):321-30.

[20] Yeagle PL, Young J, Rice D. Effects of cholesterol on (Na+,K+)-ATPase ATP hydrolyzing activity in bovine kidney. Biochemistry 1988 Aug 23;27(17):6449-52.

[21] Yeagle PL. Incorporation of the human erythrocyte sialoglycoprotein into recombined membranes containing cholesterol. J Membr Biol 1984;78(3):201-10.

[22] Klappauf E, Schubert D. Band 3-protein from human erythrocyte membranes strongly interacts with cholesterol. FEBS Lett 1977 Aug 15;80(2):423-5.

[23] Pan W. Viscoelastic properties of human mesenchymal stem cells. Conf Proc IEEE Eng Med Biol Soc 2005;5:4854-7.

[24] Zhou X, Hu D, Liu L, Wu Z, Qin J, Cai S. Effect of hypertonic saline solution on the viscoelasticities of erythrocyte membrane in rats subjected to hemorrhagic shock. Sheng Wu Yi Xue Gong Cheng Xue Za Zhi 2001 Dec;18(4):589-91.

[25] Wu Z, Zhang G, Shao K, Long M, Wang H, Song G, Wang B, Cai S. et al. Investigation on the rheological properties of hepatocellular carcinoma cells and their relevance to cytoskeleton structure. Zhonghua Gan Zang Bing Za Zhi 2001 Feb;9(1):25-7.

[26] Bausch AR, Ziemann F, Boulbitch AA, Jacobson K, Sackmann E. Local measurements of viscoelastic parameters of adherent cell surfaces by magnetic bead microrheometry. Biophys J 1998 Oct;75(4):2038-49.

[27] Lipowsky R, Sackmann E. Structure and dynamics of membranes. Amsterdam: Elsevier Science; 1995.

[28] Valberg PA, Butler JP. Magnetic particle motions within living cells. Physical theory and techniques. Biophys J 1987 Oct;52(4):537-50.

[29] Valberg PA, Feldman HA. Magnetic particle motions within living cells. Measurement of cytoplasmic viscosity and motile activity. Biophys J 1987 Oct;52(4):551-61.

[30] Lakowicz JR. Principles of fluorescence spectroscopy. 2nd ed. New York: Kluwer Academic/Plenum; 1999. Pgs 698

[31] Axelrod D, Koppel DE, Schlessinger J, Elson E, Webb WW. Mobility measurement by analysis of fluorescence photobleaching recovery kinetics. Biophys J 1976 Sep;16(9):1055-69.

[32] Goodwin JS, Drake KR, Remmert CL, Kenworthy AK. Ras diffusion is sensitive to plasma membrane viscosity. Biophys J 2005 Aug;89(2):1398-410.

[33] Li Y, Wang JJ, Cai JX. Aniracetam restores the effects of amyloid-beta protein or ageing on membrane fluidity and intracellular calcium concentration in mice synaptosomes. J Neural Transm 2007 Jun 8. Epub Ahead of Print.

[34] Ohyama H, Hiramatsu M, Ogawa N, Mori A. Age-related differences in synaptosomal membrane fluidity. Biochem Mol Biol Int 1995 Sep;37(1):133-40.

[35] Muller WE, Koch S, Eckert A, Hartmann H, Scheuer K. Beta-Amyloid peptide decreases membrane fluidity. Brain Res 1995 Mar 13;674(1):133-6.

[36] Mattson MP, Barger SW, Cheng B, Lieberburg I, Smith-Swintosky VL, Rydel RE. Beta-Amyloid precursor protein metabolites and loss of neuronal Ca2+ homeostasis in Alzheimer's disease. Trends Neurosci 1993 Oct;16(10):409-14.

[37] Parasassi T, De SG, Ravagnan G, Rusch RM, Gratton E. Quantitation of lipid phases in phospholipid vesicles by the generalized polarization of Laurdan fluorescence. Biophys J 1991 Jul;60(1):179-89.

[38] Parasassi T, Conti F, Gratton E. Time-resolved fluorescence emission spectra of Laurdan in phospholipid vesicles by multifrequency phase and modulation fluorometry. Cell Mol Biol 1986;32(1):103-8.

[39] Abdel-Mottaleb MSA, Loutfy RO, Lapouyade R. Non-radiative deactivation channels of molecular rotors. Journal of Photochemistry and Photobiology A: Chemistry 1989;48(1):87-93.

[40] Haidekker MA, Theodorakis EA. Molecular rotors-fluorescent biosensors for viscosity and flow. Org Biomol Chem 2007 Jun 7;5(11):1669-78.

[41] Rotkiewicz K, Grellman KH, Grabowski ZR. Picosecond isomerisation kinetics of excited p-dimethylaminobenzonitriles studied by oxygen quenching of fluorescence. Chem Phys Lett 1973;19:315-8.

[42] Förster T, Hoffmann G. Effect of viscosity on the fluorescence quantum yield of some dye systems. Z Phys Chem 1971;75:63-76.

[43] Loutfy RO. Fluorescence probes for polymer free-volume. Pure and Applied Chemistry 1986;58(9):1239-48.

[44] Viriot ML, Carré MC, Geoffroy-Chapotot C, Brembilla A, Muller S, Stoltz J-F. Molecular rotors as fluorescent probes for biological studies. Clin Hemorheol Microcirc 1998;19:151-60.

[45] Haidekker MA, L'Heureux N, Frangos JA. Fluid shear stress increases membrane fluidity in endothelial cells: a study with DCVJ fluorescence. Am J Physiol Heart Circ Physiol 2000 Apr;278(4):H1401-H1406.

[46] Akers WJ, Haidekker MA. Precision assessment of biofluid viscosity measurements using molecular rotors. J Biomech Eng 2005 Jun;127(3):450-4.

[47] Haidekker MA, Ling T, Anglo M, Stevens HY, Frangos JA, Theodorakis EA. New fluorescent probes for the measurement of cell membrane viscosity. Chem Biol 2001 Feb;8(2):123-31.

[48] Bangham AD, Standish MM, Watkins JC. Diffusion of univalent ions across the lamellae of swollen phospholipids. J Mol Biol 1965 Aug;13(1):238-52.

[49] Rodriguez N, Pincet F, Cribier S. Giant vesicles formed by gentle hydration and electroformation: a comparison by fluorescence microscopy. Colloids Surf B Biointerfaces 2005 May 10;42(2):125-30.

[50] Zaru M, Mourtas S, Klepetsanis P, Fadda AM, Antimisiaris SG. Liposomes for drug delivery to the lungs by nebulization. Eur J Pharm Biopharm 2007 Apr 18. Epub Ahead of Print.

[51] Noireaux V, Libchaber A. A vesicle bioreactor as a step toward an artificial cell assembly. Proc Natl Acad Sci U S A 2004 Dec 21;101(51):17669-74.

[52] Fujii S, Richtering W. Size and viscoelasticity of spatially confined multilamellar vesicles. Eur Phys J E Soft Matter 2006 Feb;19(2):139-48.

[53] Ly HV, Longo ML. The influence of short-chain alcohols on interfacial tension, mechanical properties, area/molecule, and permeability of fluid lipid bilayers. Biophys J 2004 Aug;87(2):1013-33.

[54] Notman R, Noro M, O'Malley B, Anwar J. Molecular basis for dimethylsulfoxide (DMSO) action on lipid membranes. J Am Chem Soc 2006 Nov 1;128(43):13982-3.

[55] Chin JH, Goldstein DB. Effects of low concentrations of ethanol on the fluidity of spin-labeled erythrocyte and brain membranes. Mol Pharmacol 1977 May;13(3):435-41.

[56] Ferreira H, Lucio M, de CB, Gameiro P, Lima JL, Reis S. Partition and location of nimesulide in EPC liposomes: a spectrophotometric and fluorescence study. Anal Bioanal Chem 2003 Sep;377(2):293-8.

[57] Severcan F, Suleymanoglu E, Boyar H. Turbidity studies of the effect of divalent cations on tamoxifen-model membrane interactions. Biochem Soc Trans 1997 Aug;25(3):493S.

[58] Wiseman H, Laughton MJ, Arnstein HR, Cannon M, Halliwell B. The antioxidant action of tamoxifen and its metabolites. Inhibition of lipid peroxidation. FEBS Lett 1990 Apr 24;263(2):192-4.

[59] Luxo C, Jurado AS, Madeira VM. Lipid composition changes induced by tamoxifen in a bacterial model system. Biochim Biophys Acta 1998 Feb 2;1369(1):71-84.

[60] Dicko A, Morissette M, Ben AS, Pezolet M, Di PT. Effect of estradiol and tamoxifen on brain membranes: Investigation by infrared and fluorescence spectroscopy. Brain Res Bull 1999 Aug;49(6):401-5.

[61] Custodio JB, Almeida LM, Madeira VM. The anticancer drug tamoxifen induces changes in the physical properties of model and native membranes. Biochim Biophys Acta 1993 Aug 15;1150(2):123-9.

[62] Severcan F, Kazanci N, Zorlu F. Tamoxifen increases membrane fluidity at high concentrations. Biosci Rep 2000 Jun;20(3):177-84.